Universidad del País Vasco Euskal Herriko Unibertsitatea
BILBOKO INGENIARITZA ESKOLA
ESCUELA DE INGENIERÍA DE BILBAO

**MÁSTER UNIVERSITARIO EN**

**INGENIERÍA DE CONTROL, AUTOMATIZACIÓN Y ROBÓTICA**

# TRABAJO FIN DE MÁSTER

## *DEVELOPMENT OF AN AUTOMATED STEERING SYSTEM FOR SHARED CONTROL APPLICATIONS*

**Estudiante** *Rodríguez, Arozamena, Mario*
**Director** *Zubizarreta, Pico, Asier*
**Departamento** *Ingeniería de Sistemas y Automática*
**Curso académico** *2021/22*

*Bilbao, 24, 06, 2022*

# Abstract

*Shared control techniques for Automated Driving require high-quality equipment to step up from hardware-in-the-loop simulations to real applications. Nevertheless, not every car used nowadays for Automated Driving research has a suitable steering system. This project develops a fast, reliable, and efficient two-way low-level controller of a power steering, focusing on its application in torque and position control. Hence, following this methodology, not only shared control techniques are enabled by the torque control, but also fully automated vehicles can benefit from the position control.*

# Resumen

*Las técnicas de control compartido para la conducción automatizada requieren equipos de alta calidad para pasar de simulación hardware-in-the-loop a aplicaciones reales. Sin embargo, no todos los coches utilizados hoy en día para la investigación de la conducción automatizada cuentan con un sistema de dirección adecuado. Este proyecto desarrolla controladores de bajo nivel, rápidos, fiables y eficientes de par y posición para una dirección asistida. De este modo y, siguiendo esta metodología, el control de par no sólo habilita las técnicas de control compartido, sino que también los vehículos totalmente automatizados pueden beneficiarse gracias al control de posición.*

# Laburpena

*Gidatze automatizaturako kontrol partekatuko teknikek kalitate handiko ekipamendua behar dute hardware-in-the-loop simulaziotik benetako aplikazioetara pasatzeko. Hala ere, gaur egun gidatze automatizatua ikertzeko erabiltzen diren auto guztiek ez dute direkzio-sistema egoki bat. Proiektu honek maila baxuko kontrolatzaileak garatzen ditu, azkarrak, fidagarriak eta pare eta posizio-eraginkorrak, lagunduriko direkzio baterako. Horrela, eta metodologia horri jarraiki, pare-kontrolak kontrol partekatuko teknikak gaitzen ditu. Gainera, automatizatutako ibilgailuek posizio-kontrolaren abantailak ere erabil ditzakete.*



# Key Words:

*Steering system control, DC motor torque control, DC motor position control, ADAS, Automated Driving*

# Acknowledgements

First, I would like to thank Asier Zubizarreta for his advice and support not only during this Master Thesis but during the last four years in Formula Student Bizkaia. The work you do is immeasurable.

I would also like to thank Joseba Sarabia for his support and guidelines during the daily work and for making easier the first months at Tecnalia. Besides, I would like to thank Joshué Pérez for providing me with this opportunity, as well as all the people I have worked with at Tecnalia, especially the Shared Control group, Sergio Diaz and Mauricio Marcano.

I would like to thank my parents, Iñaki Rodríguez and Cristina Arozamena, and my brother Diego Rodríguez, for their unconditional support all these years.

I would also like to acknowledge the entire Formula Student family, especially my team, Formula Student Bizkaia, for making me grow as an engineer and as a person. *Once FSB, always FSB*. But I also like to thank two teams that made me discover the field of Automated Driving, KIT KA-RaceIng and AMZ Racing ETH Zürich.

Finally, I would like to thank my cat Ariel for being by my side during the long study hours over all these years.

# Contents

# List of Tables

# List of Figures

# Acronyms

**ABS** Anti-lock Braking System

**ACC** Adaptative Cruise Control

**AD** Automated Driving

**ADAS** Advanced Driver Assistance Systems

**AEB** Automatic Emergency Brake

**AGV** Automated Guided Vehicle

**AI** Artificial Intelligence

**AV** Automated Vehicle

**CC** Cruise Control

**DARPA** Defense Advanced Research Projects Agency

**DDT** Dynamic driving task

**ECU** Electronic Control Unit

**EPS** Electronic Power Steering

**ESC** Electronic Stability Control

**FMEA** Failure Mode and Effects Analysis

**GNSS** Global Navigation Satellite System

**GPS** Global Positioning System

**HiL** Hardware in the Loop

**HMI** Human Machine Interface

**HSI** Human-Systems Integration

**IMU** Inertial Measurement Unit

**ITS** Intelligent Transport Systems

**LCA** Lane Change Assist

**LIDAR** Laser Imaging Detection and Ranging

**LKA** Lane Keeping Assist

**ODD** Operational Design Domain

**OEDR** Object and Event Detection and Response

**OEM** Original Equipment Manufacturer

**OS** Operating System

**PCB** Printed Circuit Board

**PWM** Pulse Width Modulation

**ROS** Robot Operating System

**SAE** Society of Automotive Engineers

**SI** International System of Units

**SLAM** Simultaneous Location and Mapping

**TCS** Traction Control System

**V2I** Vehicle-to-Infrastructure

**V2V** Vehicle-to-Vehicle

**V2X** Vehicle-to-X

# 1 Introduction

This document aims to describe the process and stages followed during the realisation of the Master Thesis entitled: "*Development of an Automated Steering System for Shared Control Applications*", as well as the conclusions derived from it.

The project comprehends the adaptation of an EPS (Electronic Power Steering) assembly of a Renault Clio into an automated steering system for a Renault Twizy. The proposed control system is dual in the sense that two independent and configurable controllers are designed, each using a different controlled variable. Thus, the first of them controls the motor position, whereas the second one is a torque controller. This enables different automated driving approaches besides trajectory tracking, such as Shared Control.

During this document, the stages of modelling, controller designing, and validation tests in a HiL (Hardware in the Loop) simulator are covered, concluding with the subsystem ready for assembly in the vehicle.

This project has been developed in the Automated Driving research group of the Industry & Mobility Area in Tecnalia Research & Innovation.

The document is organized as follows. In Chapter 2, the context in which this project is framed is presented. In Chapter 3, the objectives and the scope of the work are explained. Chapter 4 is used to discuss the benefits derived from the work. In Chapter 5, an analysis of the State of the Art is carried out. Chapter 6 covers the design process of the automated steering system, as well as the validation tests. In Chapter 7, the chronological allocation of the project is discussed, as well as the different tasks derived from the project. Economic aspects are discussed in Chapter 8. Finally, conclusions and future work are exposed in Chapter 9.

# Context

# 2

## 2.1 Automated Driving

### 2.1.1 Introduction

Since Carl Benz invented the car in 1886, it has become a pivotal part of our lives. Our cities, habits, ways of transportation and culture have evolved toward a car-centred society. Nowadays, the car amplifies the mobility possibilities, allowing to travel between cities, regions and even countries freely and without timetables. Nevertheless, the car has also brought several significant drawbacks, making us rethink the role of automotive transportation.

- Approximately 1.35 million people die every year from road crashes, nearly 3.700 every single day, being the leading cause of death for people aged between 5 and 29 years. Tens of millions are severely injured or disabled due to the same cause [1]. Moreover, what is worst, the majority of them are entirely preventable since 80 to 90% of them are caused by human errors [2].
- Transportation is responsible for a quarter of the EU's greenhouse gas emissions and growing. To achieve climate neutrality, a 90% reduction in transport emissions is needed by 2050. In conclusion, especially in cities, transportation should become drastically less polluting [3].
- Road congestion is one of the main problems and challenges for transport policy, inducing an estimated cost of over 110 billion € a year only in Europe. In Spain, drivers and passengers spend more than 420 million hours a year in congestion, being the majority of them concentrated in peak intervals of three to six hours daily [4].
- Numerous accessibility barriers to transportation are present in the nowadays society, i.e. physical and mental capacity to move, ability level, and security. Altogether, they prevent a part of society from using road mobility [5].

In view of these facts, the development of Automated Vehicles (AV) and Intelligent Transport Systems (ITS) is projected as a key part of the solution, as it will play an increasing role in the pollution reduction, especially in urban areas, and in congestion downsizing, with the development of smart traffic management systems [3]. Besides, it could prevent the majority of traffic accidents caused by human

factors and provide enhanced mobility opportunities. Further positive impacts such as new business opportunities, i.e., "Mobility as Service", are also projected [6]. However, further development and legal acceptance are needed to reach this state [7]. On the other hand, the automation of road transportation could also entail negative impacts, such as a disincentive to walking and biking or an increase in overall distances travelled. Another inherent risk is the inequitable access to these enhanced mobility options due to socioeconomic factors [6].

Automated Driving (AD) involves a wide variety of technologies and developments, from the most basic Advanced Driver Assistance Systems (ADAS) to more complex applications, which have evolved during the last three decades [8]. As a result, two tendencies with different approaches to the AD capabilities have arisen: Semi-automated and automated vehicles [9].

Aiming to establish a common framework and standardize the different functionalities of automated and semi-automated driving, as well as its Operational Design Domain (ODD), the Society of Automotive Engineers (SAE) published the J3016 standard in 2014 [10], last updated in 2021 [11], which establishes a level-based classification that summarizes as follows:

- **Level 0: No Driving Automation:** The driver is responsible for the entire Dynamic Driving Task (DDT), although the automated system can provide warnings or brief emergency interventions, but not on a sustained basis.
- **Level 1: Driver Assistance:** The automated system executes part of the DDT, performing whether the longitudinal *or* the lateral motion control subtask. The driver performs the remainder of the DDT, including the detection and reaction of events and objects, and supervises the automation. Furthermore, he/she must determine when the automated system engagement is appropriate and remains responsible for the vehicle's behaviour.
- **Level 2: Partial Driving Automation:** This level is almost equal to the previous one, with the exception that the automated system must perform both the longitudinal *and* the lateral motion control subtasks when engaged.
- **Level 3: Conditional Driving Automation:** The automated driving system performs the whole DDT when engaged, starting at this level. This implies that the vehicle is capable of the whole Object and Event Detection and Response (OEDR) task when operating in the ODD. The driver no longer has to supervise the automated system, but must remain alert for fallback situations like system failures or leaving the ODD.
- **Level 4: High Driving Automation:** The certification of this level entails that the automated system is capable of performing the entire DDT within the ODD.

The ODD can refer to multiple conditions, like the environment, weather, light, traffic, or speed. When performing an L4 operation, the driver does not have to supervise nor remain alert for fallback situations, but must perform the DDT if the automated driving system reaches its ODD limit.

- **Level 5: Full Driving Automation:** The maximum level corresponds to an extension of L4 to all driver-manageable on-road conditions. The vehicles could drive even without a steering wheel and pedals at this utopian level.

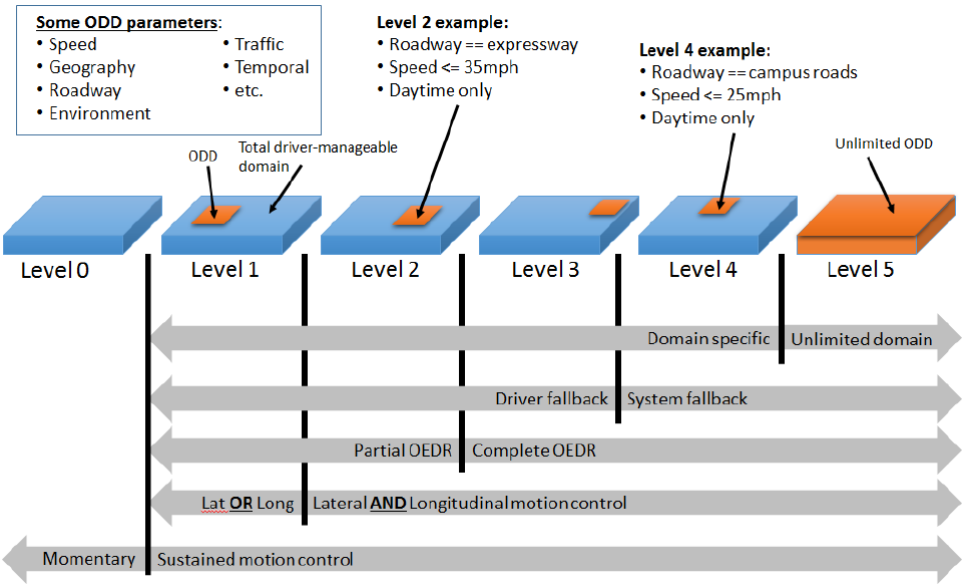


**Figure 2.1.** ODD relative to driving automation levels [11]

### 2.1.2 Historical evolution of ADAS

Although the technologies and capabilities have increased enormously in recent years, the interest in Automated Driving is not something new. Over the last decades, a great effort in the field of AD has been carried out by both the industry and academia, in many cases in terms of collaborations [12]. However, before talking about Automated Driving, it is necessary to mention Advanced Driver Assistance Systems (ADAS). These systems are considered to be one of the major contributors to the reduction of road fatalities over the last 30 years, helping to reduce fatal accidents by almost 90% [13].

Early driver assistance systems were based mainly on vehicle dynamics stabilization. They used proprioceptive sensors, which measured the internal status of the vehicle, i.e. wheel speed and acceleration [8]. One of these driving aids is the Anti-lock Braking System (ABS), patented by Bosch and first introduced in serial production in vehicles by Mercedes-Benz in 1979. This system helps to prevent the wheels from locking when braking, thereby reducing the minimum stopping distance [14]. Years later, the Traction Control System (TCS) and the Electronic Stability Control (ESC),

which supposed the entry of the electronic gyroscope in the automobile, marked a further milestone in dynamics stabilization. Studies carried out years later classified the ESC as the second most efficient safety system, only surpassed by the seat belt [15].

In the 90s and early 00s, a new generation of assistance systems was developed, focused on sensing the environment, and alerting and informing the driver, improving his safety and comfort. Thus, they use sensors classified as exteroceptive, such as ultrasonic, radar, Laser Imaging Detection and Ranging (LIDAR), cameras or Global Positioning System (GPS). Among the most noteworthy contributions are navigation systems, parking assistance, Automatic Emergency Brake (AEB) and Adaptive Cruise Control (ACC), being the vehicles with the latest classified as SAE L1 [8].

In recent years, more complex ADAS have been developed. This new generation enables entering the classification of semi-automated driving, reaching the SAE L2. Examples of these new technologies are Lane Keeping Assist (LKA), Lane Change Assist (LCA), blind spot detection, speed limit detection and adaptative lighting. Commercial vehicles with all the aforementioned features are usually referred to as Autopilots, being commercialized by companies like Tesla, Audi, BMW, Hyundai, Mercedes, Ford, Nissan, Toyota, or Honda.

In 2019, the European Parliament and the Council issued a regulation which lays the groundwork for future certifications of SAE L3 and beyond. Furthermore, it establishes the compulsory presence of a set of ADAS for new cars homologated by July 2022 and sold beyond May 2024, including [16]:

- Intelligent speed assistance
- Alcohol interlock installation facilitation
- Driver drowsiness and attention warning
- Advanced driver distraction warning
- Emergency stop signal
- Reversing detection
- Event data recorder
- Advanced emergency braking systems
- Emergency lane-keeping system

### 2.1.3 Research towards Automated Driving

The last decades have seen tremendous advances in AD. Therefore, a non-exhaustive review is here presented.

Pioneer works on Automated Driving started during the 80s. A Mercedes-Benz automated van from the Universität der Bundeswehr München, Germany, travelled more than 20 Km on closed roads, reaching speeds close to 100 Km/h in straight lines with a classical vision-based guidance system [17]. The EUREKA consortium, which included major automotive manufacturers and 120 universities and research institutes, launched the PROMETHEUS program in 1986, which focused on thematics such as sensing and actuating systems, automated vehicle architecture, Human-Machine Interface (HMI), vehicle safety and communication. Demonstrators were built around Europe to present the results of the project that lasted until 1995 [18, 19]. In the 90s in America, the "No Hands Across America" challenge saw a Pontiac minivan from the Carnegie Mellon University travel, with 98 % automated steering yet manual longitudinal control, 3000 miles (ca. 4828 Km) from Pittsburgh to San Diego [20]. LIDARs were first used in 1997 in a prototype tested on the Schiphol airport, Amsterdam. This prototype drove automatically in a dedicated lane with semaphores and pedestrian crossings, transporting passengers between the terminal and the parking [21].

In 2004, the Defense Advanced Research Projects Agency (DARPA) began organizing challenge competitions aimed at accelerating the development of automated driving technologies, the DARPA Grand Challenge. The first three editions not only marked a quantum leap in technology, but also attracted the attention of major multinationals. The 2004 and 2005 editions focused on control and navigation, taking place on closed off-road circuits. Stanford University won the second competition with a modified Volkswagen Tuareg that included 5 LIDARs, a front camera, GPS, an IMU, wheel odometry, and two automotive radars [22]. The 2007 edition changed the type of challenge, moving the setting to an urban environment in which participating vehicles had to interact with other vehicles and pedestrians, as well as follow traffic rules. As mentioned, these events attracted the attention of technology multinationals such as Google, kicking off the race to develop commercial products. [21].

In 2013 a collaboration between Daimler AG and the Karlsruher Institut für Technologie sent a Mercedes-Benz S-Class from Mannheim to Pforzheim, Germany, following the same route that Bertha Benz did with the first car back in 1888, but this time, autonomously. Even though the overall performance of the vehicle was worse than a manual driver, it reached a milestone in the sense that it encountered variable scenarios such as overland passages, urban areas, and small villages with narrow streets [23]. A few years later, in 2015, Delphi achieved the milestone of

crossing the US from coast to coast, under all kinds of weather conditions and road situations, and driving autonomously 99 % of the time.

Efforts have also been devoted to pushing the vehicle dynamics to the limits. Audi, along with Stanford University, completed in 2010 the 20 Km of Pike's Peak mountain ascension with an automated Audi TTS in 27 minutes, only 10 minutes slower than the human record [24]. Stanford University tested drifting following established trajectories with an electric DeLorean in 2020. Under drifting conditions, the vehicles operate at the limits of rear tire friction. Thus, it was intended to develop vehicle dynamics control in scenarios that push the car beyond the limits of handle [25]. The Driverless car of the AMZ Formula Student team of the ETH Zürich beat, in 2021, the time of a professional racecar driver in a narrow, cone-defined circuit [26]. Finally, high-speed tests have also been carried out in the Indy Autonomous Challenge, achieving speeds over 300 Km/h in an oval circuit in 2022 [27].

Unfortunately, the first fatality involving an AV was occurred in 2016, when a driver of a Tesla misused the technology and did not respond in time to the take-over request [28]. During the same year, Google's car did not recognize a pedestrian who was crossing the street at night and was killed [29].

Nowadays, the most advanced AVs can be classified between SAE L2 and L3. With the aim of developing and testing technologies that can settle down L3 and achieve L4 or even L5, a great number of alliances have been generated. Companies like Honda, Toyota, Ford, Mercedes, BMW, Volvo, Volkswagen, Tesla, Google, or Amazon have reached agreements with, or buy, startup companies developing related technology. Besides, companies like Uber, Argo AI, Aurora, nuTonomy, Zoox, Cruise or Waymo are already testing automated taxi services in specific areas.


(a) Universität der Bundeswehr München automated van


(b) Stanford's vehicle in DARPA Grand Challenge 2005


(c) Audi TTS

(d) Stanford's DeLorean


(e) AMZ Formula Student Driverless


(f) Waymo automated taxi

**Figure 2.2.** Automated Vehicles

## 2.2 HADRIAN Project

The development of this Master Thesis is framed under the EU-funded HADRIAN project (H2020 under grant agreement No.875597), which stands for Holistic Approach for Driver Role Integration and Automation Allocation for European Mobility Needs. The project investigates the definition of safe and acceptable driver roles for higher levels of automated driving [30].


**Figure 2.3.** HADRIAN Project [31]

Widespread implementation of fully automated driving seems unlikely during the next ten years, at least on the European roads. Therefore, the human will likely remain a driver and will have to interact with the automated vehicle. For instance, in an SAE Level 3 [11] vehicle, the human role is to remain attentive in case of a takeover request. This new role dramatically differs from the traditional role of humans in Human-System Integration (HSI), which allocates the human in complete control of the system [30].

Several research works have been sceptical about the potential consequences of maintaining the human as a supervisor in automated vehicles and the associated issues [30, 32, 33, 34, 35, 36]:

- **Driver out of the loop:** The attention paid to the driving task by the driver is reduced after long periods of continuous automated driving. This could cause issues when the human needs to regain situational awareness and control of the vehicle.
- **Trust-calibration:** Potential dangerous situations can occur when the human overestimates the capabilities of a concrete ADAS, for example, when it is driven to the limit and suddenly disconnects. This situation could also lead to the opposite state of under-trust. As a result, only with time and experience do the users learn to calibrate their trust to the automated functionalities.
- **Humans are good controllers, but bad monitors:** Humans tend to perform better when performing active control tasks, which can be perceived as rewarding, than repetitive monitoring tasks that can easily cause distractions.

- **Understanding of intent:** To ensure safe traffic operations, it is critical that the different actors involved understand the intentions of each other, for example, during an AD level transition. How to make intelligent systems that correctly infer intent from humans and share their own is currently a big challenge.

- **Mode awareness:** Under normal circumstances, it is difficult to differentiate by the vehicle behaviour whether an AV is operating in levels 2, 3 or 4, which can lead to potential risks.

Under these premises, the challenge is to design an interface who provides enough information to the human driver, who may be unaware of what is happening, ensuring a fast response when needed but without overloading the driver with information [37]. Hence, the HADRIAN project, and thus, this Master Thesis, focuses on researching the human mobility needs joining influencing factors from four different viewpoints: Goals, Environment, Opportunities and Capabilities in a holistic approach. This means that the vehicle is no longer the only actor expected to address the challenges of automated driving, as in traditional Automated Driving approaches, but a part of a mobility service also composed of the driver, the environment, the infrastructure and the nearby vehicles. The project focuses on three use cases, consisting of an elderly driver, a truck driver and an office worker driver, each of them having different mobility needs [30, 31].

The solution proposed is the so-called *HADRIAN f*-HMI (fluid HMI), "*a multisensory, omnipresent, and omnidirectional system that constantly monitors the driver, his activities and attentional levels to update a driver digital twin model*". This proposal aims to increase situational awareness, minimize obtrusiveness, and preserve the cognitive spare space capacity for takeover requests, ensuring a smooth and safe transition of control.

This way, the solution intends to enable the implementation of AD functions such as the sustained monitoring of the driver and the environment, the control management, informing the driver about the current and future states, as well as learning from him, communicating outside the vehicle (Vehicle-to-X, V2X), adapting to the driving style or even the tutoring of manual drivers towards increasing automation levels [31, 37].

The *HADRIAN f*-HMI consists of four key elements:

- **The HADRIAN fluid tutoring system:** A training method for drivers to develop a model of the automated vehicle and to increase the transparency and acceptance of automated vehicles, as well as to generate a calibrated trust. Derived works are being done in [38].

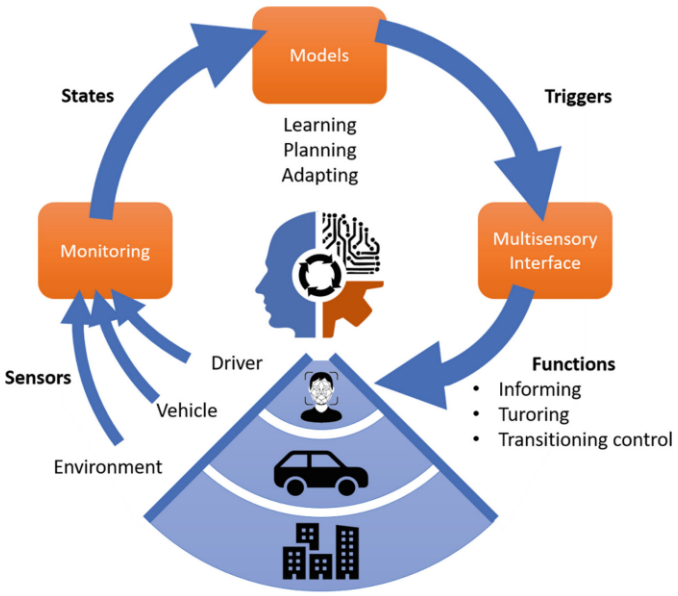


**Figure 2.4.** Scheme of the Fluid concept proposed by [37]

- **The HADRIAN Fit2Drive system:** It intends to detect dangerous driver states such as distraction or fatigue and to anticipate unsafe situations. Derived works include [39, 40, 41].
- **The HADRIAN Head-Up Display:** Highlights critical information on a window-like display, intending to increase safety. Derived works include [42, 43].
- **The HADRIAN haptic steering wheel feedback algorithm:** Combines the use of shared control algorithms for collaborative driving and transitions between manual and automated driving with active and passive signalling. Derived works include [44, 45, 46, 47, 48].

The project outcomes will be tested on different demo vehicles, such as a large passenger vehicle, a van and the Tecnalia's automated Renault Twizy. However, the Twizy currently presents a problem due to the mechanical design that hinders the deployment of shared control algorithms. The steering wheel is currently actuated through a motor with a speed reducer of a 200/1 ratio and drives the steering column through a belt [49]. It is suitable for fully autonomous driving but generates non-linear behaviours when executing shared control algorithms. Besides, due to the speed reducer, manual or semi-automated driving requires a significant effort, which is unpleasant and incompatible with the vision of the HADRIAN project.

This leads to the specific context in which the project is placed, one of the future works derived from the PhD Thesis of Dr Mauricio Marcano [47] while aligned with the ongoing PhD Thesis of Joseba Sarabia: The development of an automated steering system that can substitute the current one and, therefore, enable the test and validation of shared control algorithms on a real vehicle.

**Figure 2.5.** Tecnalia's automated Renault Twizy

## 2.3 AUDRIC2 - Automated Driving Framework

The module-based automated driving framework presented in [50] is currently the literature reference. It comprehends six blocks with well-defined functions in the workflow of an AV.

- **Acquisition:** This module collects data from the sensors and processes them accordingly. This includes proprioceptive sensors, which collect information about the state of the vehicle or the driver, such as IMUs or encoders, and exteroceptive sensors, which collect information about the environment, such as radar, cameras or LIDARs.

- **Perception:** In this stage, the data received from the Acquisition module is used to generate information about the environment and the ego-vehicle. During this stage, Simultaneous Location and Mapping (SLAM) techniques are used to locate the ego-vehicle, whereas Artificial Intelligence (AI) and sensor fusion techniques are used to detect and classify roads and obstacles.

- **Communication:** This module provides information from other vehicles (Vehicle-to-vehicle, V2V), the infrastructure (vehicle-to-infrastructure, V2I) or an external entity (V2X). This includes communication with mobile networks or even Global Navigation Satellite System (GNSS), which improves positioning accuracy.

- **Decision:** This layer is the core of the architecture. It receives processed information from the perception and communication modules and decides the dynamic behaviour that the vehicle should have. In other words, it determines the trajectory, allowing to interact with unexpected situations. It is composed of three sub-modules:

  - Global Planning: Generates an accurate global path considering information from a map file.

  - Local Planning: Its function is to improve the trajectory by adding smoothness using different curves such as Bézier [51, 52]. Therefore, improves the comfort of the passenger.

  - Behavioural Planning: Changes the trajectory depending on the dynamics of the considered manoeuvres, i.e. overtaking, obstacle avoidance and lane changes.

- **Control:** This stage receives the path to follow from the decision module and ensures it is executed correctly, comparing it to the current state. Within this

phase, control algorithms such as Model Predictive Control (MPC) [53], Fuzzy Logic or PIDs have been implemented.

- **Actuation:** This layer refers to the vehicle actuators such as the throttle, brake pedals, and steering wheel. It also includes the low-level control of such actuators, which receive the desired actuator state from the control module.

The framework was designed originally for automated driving. However, the shared control schema modifies the architecture, as it requires four more sub-modules distributed along the decision, control, and actuation modules, as indicated in [47].

- **Decision:** Receives the addition of an arbitration sub-module which harmonizes the driver and automation inputs, along with a fallback system which provides appropriate feedback.
- **Control:** A shared-controller sub-module is added, which uses torque or force as the controlled variable instead of the position.
- **Actuation:** Requires the implementation of additional instrumentation. Furthermore, it affects the shared control scheme depending on the actuation mechanism used (coupled or steer-by-wire).

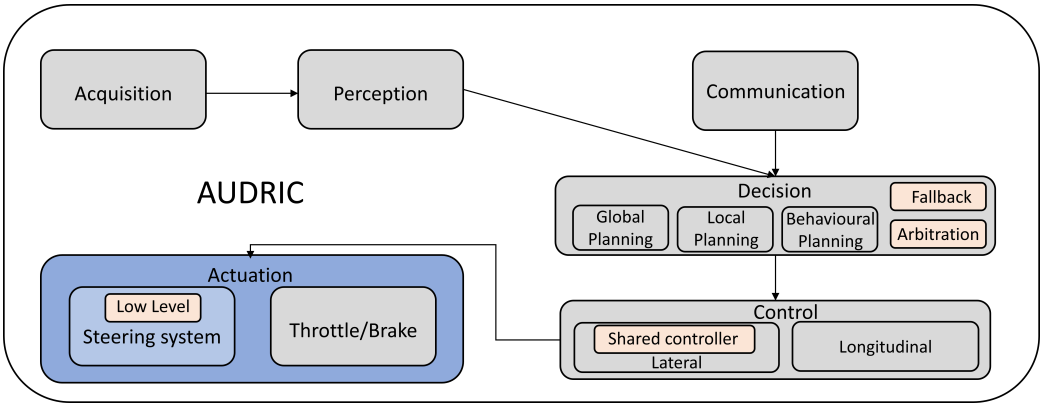


**Figure 2.6.** Automated Driving Framework reviewed in [50] and adapted in [47]

This Master Thesis focuses on the Actuation module, in particular in the steering system, adapting it to fulfil the necessities of shared control but also maintaining the automated driving capabilities.

Under the name of AUDRIC, this modular framework was first implemented in [54] in 2017. Since then, it has been implemented on different platforms such as the aforementioned automated Renault Twizy, buses, forklifts, Automated Guided Vehicles (AGVs) or simulators, which highlights its modular capacities. The newest version, AUDRIC2 [55], was released in 2021 and is capable of being deployed within Windows OS in MATLAB/Simulink and within Linux using ROS.

# 3 Objectives and scope of work

The main objective of the project is to develop an automated steering system capable of being mounted in a Renault Twizy. This makes a substitution of the current solution possible, which, as stated in Chapter 2, has a mechanical design that makes manual and shared driving unpleasant.

The achievement of the principal objective entails the attainment of two partial objectives needed to fulfil the capabilities to which the solution is restricted. These are the development and validation of position and torque control, which are needed, respectively, for fully automatic driving and shared control.

Furthermore, as part of the shared control framework, the platform needs to be capable of executing the so-called Haptic Icons. This feature serves as a communication interface between the vehicle and the driver and is composed of sequences of steering wheel vibrations with different amplitudes and frequencies.

The scope of the project is defined as follows:

- The development of the automated steering system involves neither mechanical nor electrical design. This means that the work is focused on the automation of an existing and commercial Electronic Power Steering (EPS), in this case, from a Renault Clio.
- On the other hand, the additional sensors needed and the electronic hardware like a motor controller do belong to the scope of the project. Nevertheless, the integration of commercial hardware is preferred over electronic design when possible.
- Both controllers need to be validated with the actual steering assembly but outside the vehicle. This means that a simulator consisting of the steering wheel, the steering motor and the steering shaft is mounted, enabling Hardware-in-the-Loop testing.
- Finally, the assembly of the system in the vehicle and the consequent fine-tune of the solution escape the scope of the work and, therefore, are not included in this document.

# Benefits of the work

# 4

The realization of the project entails different benefits, which can be approached from different perspectives.

From a technical point of view, the project has the following benefits:

- First, a methodology for automating a commercial electronic power steering is here presented, which contributes to enabling the automation of daily-use vehicles.
- The torque control of an automotive steering system allows the development, testing, and improvement of shared control algorithms in actual road vehicles, which are very demanding in terms of hardware.
- The proposed solution facilitates a configurable control type. Although enabling shared control algorithms are the principal motivation, not only a torque control is developed, but also a position control.

On the economic front, the project has the next main benefit:

- The methodology enables an alternative road for non-OEM centres to research and develop automated driving applications, since it can be applied to prototypes and to non-automated vehicles.

Last but not least, the project provides the following social benefit:

- The proposed methodology facilitates the development and testing of different approaches of automated driving, which ultimately will contribute to a future with safer and more inclusive road transportation.

# 5 State-of-the-Art

This chapter covers an analysis of the studied State-of-the-Art. First, an analysis of shared control is carried out. This analysis aims to understand the needs of the high-level control for which the steering system is designed. Then, an analysis of the DC motor control techniques for Automated Driving takes place.

## 5.1 Shared control

### 5.1.1 Cooperative control

In the field of Human-Machine cooperation or cooperative control, both the human and the machine can affect the output of the system. According to [56, 57], there are five main branches of cooperative control, depending on the role and the relationship between the human and the automation.

- **Guided control:** The human has the final authority and the responsibility of the task execution, whereas the machine helps him/her with visual, acoustic or haptic aid. Navigation systems are an example of guided control [47].
- **Supervisory control:** As opposite, the machine is in control, whereas the human supports the task with tactical commands. One of the best examples is teleoperation, where full robot autonomy is not needed, but the ability to achieve some local goals while the human sets high-level goals [58].
- **Traded control:** Both the human and the machine have total control of the task, but at different times [59]. An SAE L3 vehicle falls into this category, since the vehicle can perform the entire driving task, but so can the driver when disengaged.
- **Allocation control:** The main task is divided into various subtasks. The human is responsible for a specific input subset, while the machine provides the rest of the input [60]. An SAE L1 vehicle with ACC is an example of allocation control.
- **Shared control:** In this mode of cooperative control, there is a consensus between human and automation. Both of them control the task at the same time, together [47]. A Lane Keeping Assistance could be an example of shared control.

There is currently a great deal of debate in academia about what kind of cooperative control best suits the Automated Driving problem [59]. Researchers like Abbink [61] and Marcano [47] defend shared control, while traded control is proposed by researchers like De Winter [62]. Both of them have advantages and disadvantages and suit better in different applications. Nonetheless, shared control is prospected to be massively implemented earlier since it maintains the driver in the loop. As it has been said during this document, the scope of the project is to develop a low-level control for shared control, which will be the focus from here on.

### 5.1.2 Definition

The term shared control has been a point of confusion in the literature since the 70s, being employed for different approaches to cooperative control [63]. Nevertheless, currently, there is a widely accepted definition proposed by Abbink in [58]:

> *"In shared control, human(s) and robot(s) are interacting congruently in a perception-action cycle to perform a dynamic task that either the human or the robot could execute individually under ideal circumstances."*

For better understanding, metaphors that describe the roles and relationship between the human and the machine are usually used and can be found in the literature. The most famous is the rider-horse metaphor, also known as H-Metaphor, which was proposed by [64]. This metaphor compares the task of cooperative driving in a shared approach with the activity of riding a horse. When riding, horses and humans can sense each other through the reins, which is a haptic channel. When driving, the haptic channel becomes the steering wheel or the pedals. The rider gives more liberty to the horse if he loosens the reins, or the opposite, he can tighten them to exert more control. Systems based on shared control follow the same approach, providing a continuous spectrum of authority in which the automation assists the driver. Further metaphors like the instructor-student during aviation lessons, the joint-carrying of an object or the parent-child relationship when learning to bike are also found in the literature [63].

### 5.1.3 Application of shared control in AD

Shared control can be applied in different automated driving tasks, which can be hierarchically classified into three levels [58].

- **Strategic Level:** Refers to planning and task set adaption. This includes how to go from one place to another.
- **Tactical Level:** Corresponds to the decision making and task management, such as deciding to overtake or to change the distance to the vehicle in front.

- **Operational Level:** Interacts with the actuators, setting the exact command that the low-level control must accomplish. Most shared control algorithms in the AD domain belong to this category [63].

The literature reveals two differentiated applications of these techniques. On the one hand, works related to longitudinal control can be found. Hence, most of them use haptic pedals, which can interact with the driver through force. Use cases include car-following [65], legal speed limits communication, and ecological driving assistance. Bosch also commercializes a haptic gas pedal that can provide counter-pressure, knocking and vibrations to the driver's foot. The company claims that these features can be used to indicate the recommended gear or to ease coasting.


**Figure 5.1.** Bosch haptic gas pedal

Nevertheless, most shared control applications focus on lateral control. Therefore, the steering wheel is the haptic channel in these applications, interacting through torque. Companies like Audi and Mercedes-Benz commercialise this kind of steering wheel. The most common and researched applications of lateral shared control include lane-keeping [66], obstacle avoidance [67], adaptive co-pilots [68], and overtaking manoeuvres [47]. However, most of them have been tested only in Driver-in-the-Loop simulations, and are yet to be implemented on real vehicles. As stated before, the aim of the project is to develop a low-level controller that makes this possible.

**Figure 5.2.** Haptic steering wheel

### 5.1.4 Arbitration

One of the critical aspects of shared control, especially in the applied field of Automated Driving, is the arbitration system. The arbitration system determines the share of the final control output that corresponds to each of the agents, i.e. the human and the machine. This harmonisation system is time-critical, since it needs to synchronise the control outputs of each agent [69, 70]. Several variables, like the driver state, the time to a possible collision, the disparity between control outputs or the time to lane crossing, have been studied for the arbitration system [47]. Hence, if a great authority is given to the human, the automation would barely interfere with the driving task. If, on the other hand, most of the authority belongs to automation, the effect of the human behaviour would be lowered.

How to properly implement this concept has been worked on in the literature by several authors with different approaches. Anderson proposes a linear function depending on the calculated instantaneous threat [71], Liu [72] and Marcano [73] included Fuzzy logic to determine the authority. The latest also included the authority calculation as a variable in an Model Predictive Controller (MPC) [47].

### 5.1.5 Shared control frameworks in AD

Two defined frameworks, depending on the mechanical actuation mechanism, have been found in the literature for the automotive domain.

- **Uncoupled shared control:** The vehicle output and the interaction channel with the driver are not physically coupled. This means that an intermediate controller post-processes the driver's command and complements them in accordance with the automation goal. Therefore, the final authority is given to automation. This type of actuation implies that the vehicle output does not need to match the desire of the driver, which may cause rejection by the population. Nonetheless, under normal circumstances, the system should perform virtually coupled. This operation is also known as drive-by-wire [63]. Many research efforts have been made, focusing on MPC in applications like obstacle avoidance [74], or even Lyapunov functions, in lane departure avoidance [75] etc.

- **Coupled shared control:** In this framework, the automated system acts through force feedback, giving control actions to the guidance system. In this case, the control interface (steering wheel or gas pedal) is mechanically coupled to the guidance system, which is the direct responsibility for the vehicle trajectory. This means that the final authority is given to the driver if he or she applies sufficient torque [63, 76]. MPC and fuzzy controllers have been proposed for the tasks of highway driving [77], or even a stochastic

game-theoretic approach for lane change assistance [67]. This is the use case for traditional haptic guidance systems, and also for this Master Thesis, since it is the approach followed by the Renault Clio steering system.

In conclusion, shared control techniques usually rely on advanced controllers like MPCs for computing the desired torque at each moment. Therefore, the low-level controller needs to ensure that the motor follows the desired reference fast enough. Otherwise, the effectiveness of the shared control would be jeopardized. It is relevant to mark that the references provided by the high level are usually smooth enough for the motor to be capable of following them. As a result, the low-level controller "only" needs to ensure that the motor remains in the desired state, minimizing possible disturbances.

## 5.2 Motor control

Most of the current research efforts in motor control for Automated Driving applications focus on Drive-by-Wire technologies. Even though it is not the use case of the project, an non-exhaustive analysis is first carried out. Then, an analysis of position and torque control for coupled topology is followed.

### 5.2.1 Drive-by-Wire

In the automotive industry, Drive-by-Wire technology refers to the use of actuators and sensors to perform functions traditionally achieved through the use of mechanical control systems. The use of this technology allows for increased vehicle efficiency, thereby reducing wear and tear and environmental impact. This actuation system is used in automated driving technology, which is gradually becoming a reality. However, it is not new, as it has been used in aviation for decades [78, 79].

Drive-by-Wire, or simply By-Wire, comprises three main branches. Electronic throttle control or Throttle-by-Wire, brake control or Brake-by-Wire and steering control or Steer-by-Wire. The latter is one of the major challenges in the field of Automated Driving, and is, therefore, an area on which a great deal of research is focused [80]. However, all types of By-Wire technology are based on the use of sensors to collect information, which is sent to processing units or ECUs (Electronic Control Units). Those devices are responsible for generating a setpoint that an actuator is charged with carrying out.

Throttle-by-Wire is the most established of the three technologies [81] and the easiest to find in today's vehicle fleet. A sensor located in the accelerator pedal replaces the mechanical connection to the accelerator in vehicles implementing this technology. The advantages of this technology include, in addition to reduced wear and tear, the enablement of control technologies that increase efficiency [81] or even take over the longitudinal movement of the vehicle autonomously. Examples of such technologies are cruise control, traction control and stability control [79].

The other technology that allows a vehicle to be driven longitudinally is Brake-by-Wire. Like Throttle-by-Wire, it eliminates the hydraulic brake components and replaces them with sensors and actuators that control the vehicle's brakes. This reduces reaction time, vibration, size and weight of the braking system [79].

Finally, the "Steer-by-Wire" controls the vehicle laterally. For this purpose, an actuator controls the steering, the position of which can be known at any time by means of sensors such as encoders. This technology enables the use of control techniques, which, among other advantages, lead to a reduction of the driver's steering effort,

increase stability, or even control the vehicle's lateral behaviour autonomously, continuously controlling the movement, or shared, allowing the vehicle to react to external dangers and threats [82].

Currently, the reliability of the "By-Wire" technology is one of its main problems when implemented in today's cars, as purely mechanical systems are considered to be less prone to failure [79].

Focusing on Steer-by-Wire, a search in the literature shows that applications of force feedback have been developed [83]. Other works focused on using the steer-by-wire approach to change the vehicle handling characteristics [84]. Furthermore, efforts to develop fault-tolerant control have also been dedicated [85].

### 5.2.2 Coupled topology

Most traditional vehicles belong to this category, since they were designed to be driven manually. The driver exerts torque to the steering wheel, which is connected through the steering shaft to the steering rack, which ultimately modifies the wheel angle. The torque exerted needs to overcome all resistant torques to displace the steering wheel, including the self-aligning torque, which is dependent on the vehicle speed and tends to centre the wheels. However, most cars rely on Electronic Power Steering to decrease the effort needed to move the steering system.

The development of position control for this topology has been a topic of interest since the pioneer works on Automated Driving. Most solutions found are based on PID controllers, which are well-known for being simple but effective. The controller tuning is left as the main topic of research. Sotelo developed a tuning method based on the desired response, and the Ackermann vehicle model [86], whereas works like [87] applied the Ziegler-Nichols method, other works tuned the controller heuristically [88]. Adaptive PIDs based on evolutionary algorithms have also been proposed by authors like Zhao [89]. In [90] authors even proposed the use of Fuzzy logic as the low-level controller.

As it has been exposed, the use of a PID-based controller for the low-level position control of the motor seems the most established option due to its simplicity and performance.

On the other hand, there is a lack of work related to torque or current control of brushed DC motors for Automated Driving applications. In the literature, position and speed control of DC motors are widely analysed areas, being PIDs the most relevant approach. In brief, among the few related works are Abeykoon [91], who proposed a simple PID-based current control, and Saifia [92], who opted for Fuzzy control for an EPS, which allowed him to consider power limitations.

As can be seen, not many related works could be found, probably because DC brushed motors are mainly used on speed and position control applications, leaving torque control for other electric motors such as the BLDC. Consequently, it was opted to implement the widely-used PID.

# 6 Design of the automated steering system

## 6.1 Overall view of the proposed solution

As stated in section 3, the ultimate goal is to replace the steering system of the automated Twizy with Renault Clio's one. The car needs to be driven in a fully autonomous mode, which requires a low-level position control, but also in a shared control mode, resulting in a need for low-level torque control.

Figures 6.1 and 6.2 summarize the designed solution and its integration in the Actuation module of the Automated Driving framework of [50] and evolved by [55, 47] exposed in section 2.3.

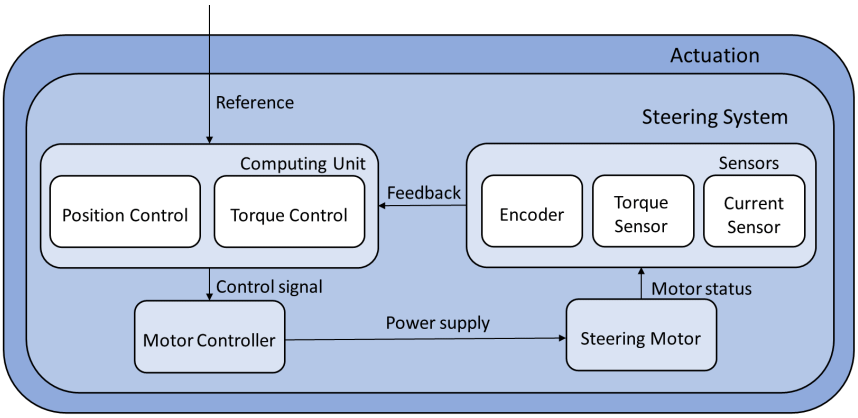


**Figure 6.1.** Overall view of the proposed solution

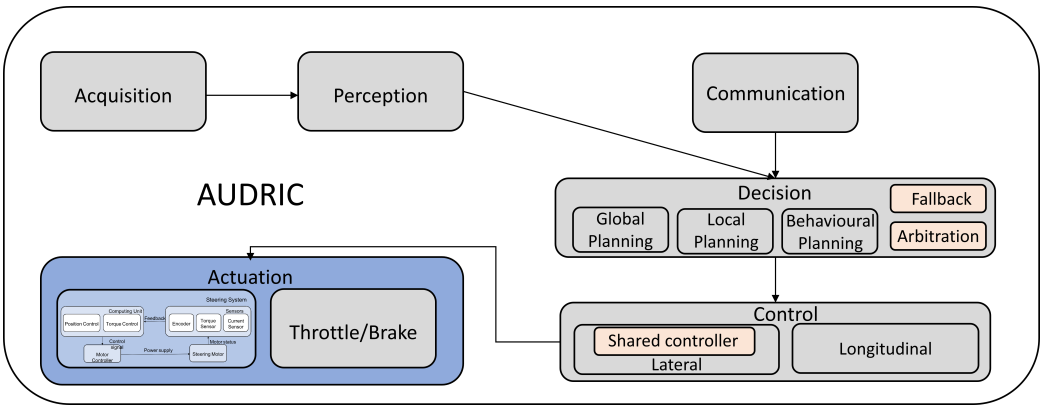


**Figure 6.2.** Integration of the proposed solution in the Automated Driving Framework

## 6.2 Design requirements

The solution is intended to be integrated in an automated vehicle, which means that the low-level control is constrained by the current design of the higher-level controls. As a result, the solution must adhere to the following requirements:

The current high-level position control loop runs at a sample time of 10 ms. The high-level loop needs a significantly faster low-level control to consider it transparent, resulting in a sample time requirement of 1 ms. On the other hand, the current high-level shared control runs at a sample time of 10 ms at the simulator. Following the same reasoning, at least a 1 ms sample time is needed for the low-level torque control.

The steady-state error must be maintained below $1.5^o$ in the case of position control and 1 Nm in torque control. These requirements allow, respectively, an appropriate lateral control of the vehicle and a precise vehicle-human interaction.

Real-time capabilities are needed in both controllers to ensure good integration with the rest of the automated driving architecture. Developing a refined control that cannot be executed in time is pointless.

Besides, the shared control application has some specific requirements for torque control. At least the capability to exert 10 Nm is required to ensure enough capacity to make corrections. Furthermore, the torque control must minimize the ripple since it generates vibrations transmitted to the driver through the steering wheel. In addition, one of the features of shared control is the implementation of haptic icons. In other words, intentional vibrations of different frequencies and amplitudes intend to serve as communication between the car and the driver. This means that the hardware used needs to be capable of generating this feature.

Last but not least, the mechanical packaging of the solution is also critical since it is meant to be mounted on a real car, which suffers forces and vibrations, and has limited space.

In summarising, the requirements remain as follows:

**Table 6.1.** Design requirements

| Requirement | Position Control | Torque Control |
|---|---|---|
| Sample time | 1 ms | 1 ms |
| Steady-state error | $\leq 1.5\ ^o$ | $\leq 1$ Nm |
| Real-Time | ✓ | ✓ |
| Minimum rated torque | X | 10 Nm |
| Low vibrations | X | ✓ |

## 6.3 Reverse engineering

The starting point is the EPS (Electronic Power Steering) of a Renault Clio, composed of part of the steering shaft, to which the steering wheel and a geared motor are coupled. At that time, it was known that it was a DC motor, but there was no further information available. This obscurantism is widely common when using parts that belong to commercial car models, as they are meant to serve only as a plug & play replacement for broken pieces. Hence, any development that aims to use this kind of automotive parts requires a reverse engineering effort to model the dynamics systems, and to obtain information about sensors and electronic systems. Furthermore, the original encoder and the steering wheel torque sensor are available, both without any kind of user information or datasheets.

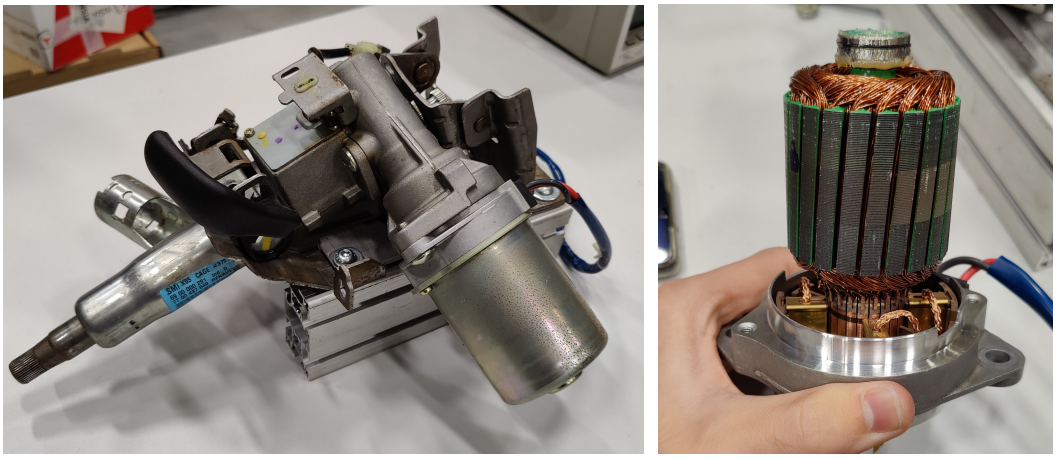

**(a)** DC Motor and steering shaft assembly **(b)** DC Motor disassembled

**Figure 6.3.** DC Motor

Thus, the first efforts are focused on obtaining the operating mode of the sensors, to then being able to obtain the dynamic model of the motor.
The encoder is designed to be attached on an axis, which means that the rotatory part is fixed on the shaft with a steering wheel coupler, and the static part is attached to the stationary part of the assembly shown in Figure 6.3. This means that the original steering wheel of the Renault Clio is also needed.

### 6.3.1 Original encoder

First, the four-wire encoder is disassembled, aiming to search for known components that could help to identify the type of output. The result is the location of a CAN transceiver, which means that the wires correspond to the power supply, CAN High and CAN Low. An analysis made with a CAN bus monitor showed that the encoder sends a new message with the angular position each 10 ms, which is too slow and does not meet the requirements. However, it is used during the project development,

leaving the upgrade to a faster one for the vehicle assembly. The Twizy already has a faster encoder that, due to planning issues, could not be extracted for use.

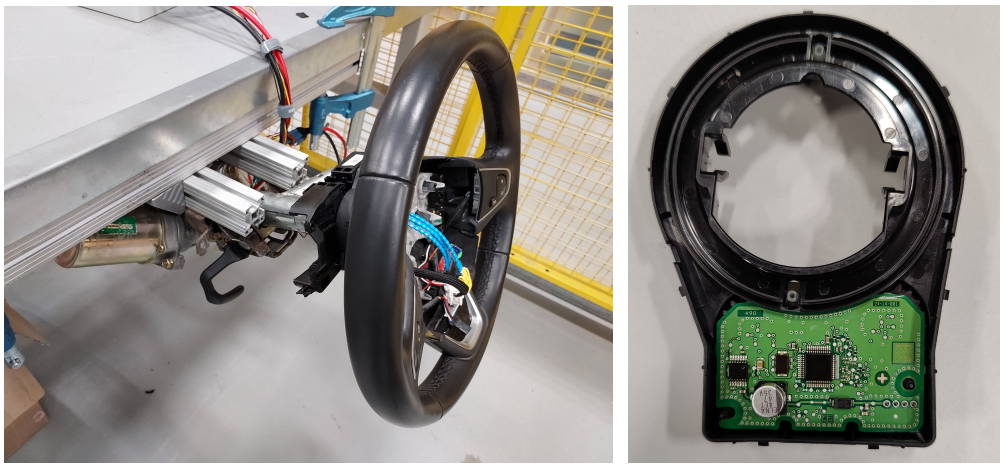

**(a)** Encoder attached to the steering wheel **(b)** Disassembled encoder

**Figure 6.4.** Original encoder of the Renault Clio

Besides, due to the mechanical coupling mechanism of the encoder currently being used on the car, which works at a 1 ms rate, it is not possible to purchase another one to use it without duplicating a big part of the mechanical steering system, leaving the aforementioned encoder as the only option.

### 6.3.2 Steering wheel torque sensor

Once the encoder's operation is known, efforts are focused on the steering wheel torque sensor. The sensor is integrated into the motor assembly and has a four-wire connector. Related work with the assembly done by [93] shows that the sensor is, with a high probability, based on the magnetoresistive effect. This means that rotation of the steering column provokes a changing magnetic field, which changes the value of a resistor. Nevertheless, how the sensor internally works is not as relevant as knowing how to condition its output signal, since as said, it's an assembled commercial sensor. However, it is relevant to consider that the measured torque does not correspond with the motor torque, but with the one applied to the steering wheel. Thus, a current sensor is needed to calculate the motor torque. From the connector, two of the wires belong to the power supply, whereas the remaining two form a redundant analog current output. In order to convert the signal into a voltage one, a simple electronic circuit consisting of a current to voltage converter is built.

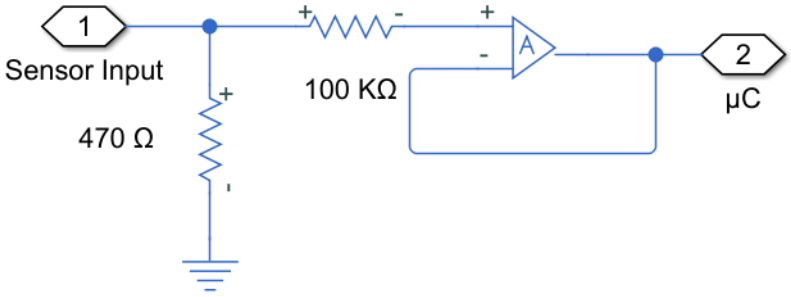


**Figure 6.5.** Torque signal conditioning circuit [93].

The next step after preparing the electronic circuit is to obtain the sensor's response under different torque values. To do so, the motor is powered on with an adjustable DC power supply and stalled with a dynamometric wrench. Repeating this procedure at different voltage values produces different stall torques. Finally, annotating the torque read at the wrench and the voltage output of the sensor allows to create a calibration line. Nevertheless, the motor is stalled using a bolt attached to the wrench, so it can only be turned clockwise, otherwise, the bolt would loosen. The calibration results are now presented:

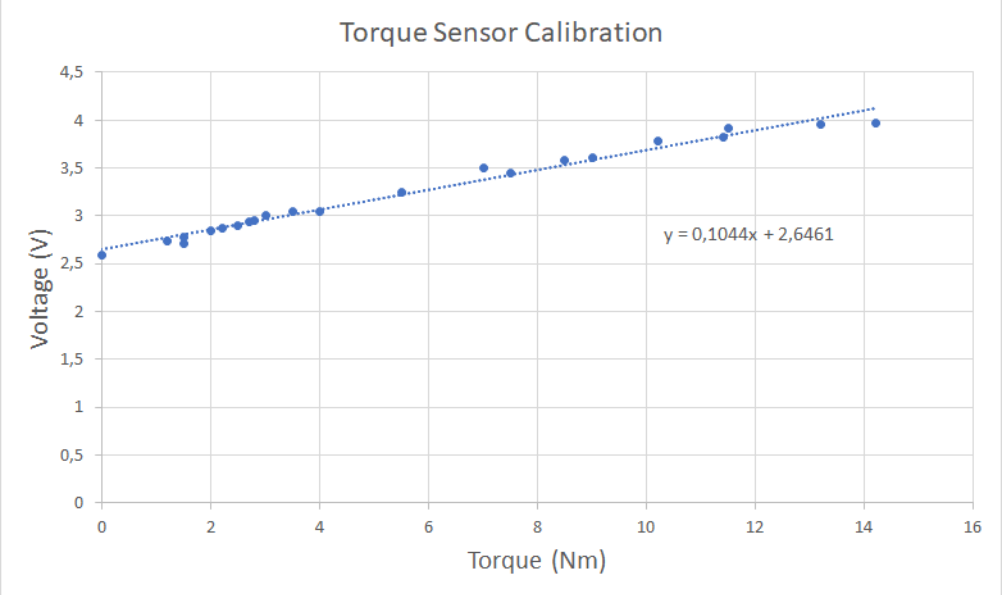


**Figure 6.6.** Calibration line of the torque sensor.

As can be seen, a 2.5 V value corresponds to 0 Nm, and the output is quite linear. An assumption of under 2.5 V output for anticlockwise applied torque seems now feasible, which is corroborated by applying a manual torque.

### 6.3.3 Current sensor

Shared control applications need to actuate on the motor torque, which is affected not only by the driver but also by the vehicle dynamics. As said, the torque sensor of the assembly only measures the first one.
In a DC Motor, the torque is directly proportional to the current:

$$\tau(t) = K_T \cdot i(t) \tag{6.1}$$

Hence, a current sensor is needed to implement a torque control loop. Current can be measured with different kinds of sensors. Some of them are the following:

- Shunt Resistors: One of the easiest ways to measure current. A low-value resistor is placed in series with the current flow intended to be measured. Thus, the current flow is directly proportional to the voltage drop across the resistor. However, a device like an optocoupler is needed to achieve galvanic isolation.
- Hall Effect Sensors: This technology is based on the voltage generated when a magnetic field cross a conducting material in which a current flows, due to Lorentz forces. In addition, a current flow creates a magnetic flux, the density of which is proportional to the amount of current flowing.
  The open-loop hall effect current transducers implement this technology in the simplest way. The magnetic field created by the current that wants to be measured is concentrated by a magnetic core. This core has a gap cut through it, in which a thin sheet of conducting material supplied with a control current is located. The hall effect is here produced, resulting in a voltage which is then measured. Hence, it is an intrinsically galvanic isolated sensor, and there is no need for optocouplers.

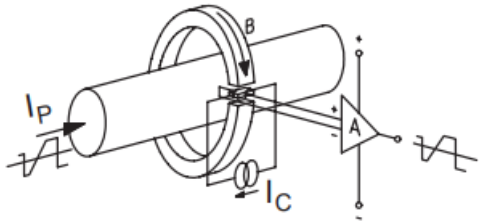


**Figure 6.7.** Conversion of the primary current into an output voltage [94]

A Hall effect sensor of the manufacturer LEM is selected, namely the HX 15-P/SP2, which has the following characteristics:

- Measuring Range: $\pm$ 45 A
- Supply Voltage: 12 V Unipolar

- Output Signal: 0 to 5 V with 2.5 V corresponding to no current
- Accuracy: 1 %
- Operating Temperature: [-25ºC to 85ºC]

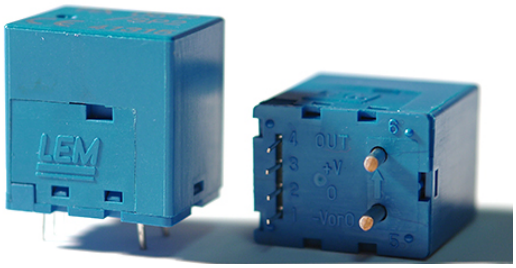


**Figure 6.8.** LEM HX 15-P/SP2.

As stated in 6.1, the motor torque is directly proportional to the current. A similar experiment to the one made with the torque sensor is carried out to calculate the $K_t$, stalling the motor with a dynamometric wrench and measuring the output current. First, the current-voltage relation is tested. An adjustable power supply is used to set different current levels, while the voltage output is noted. The result is now presented:

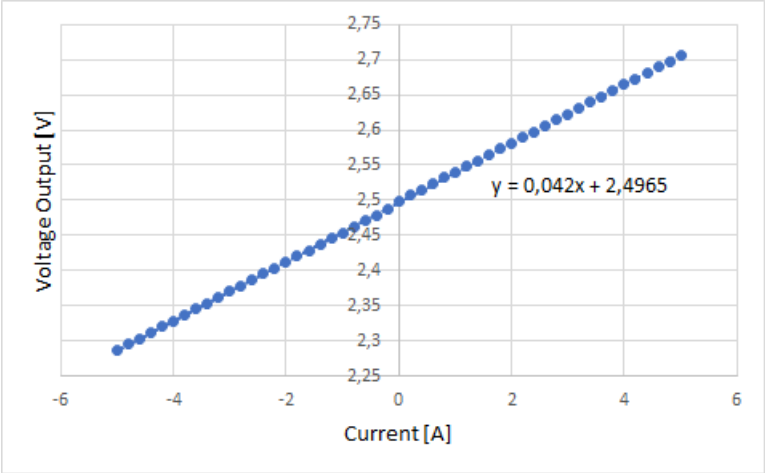


**Figure 6.9.** Output voltage of the current sensor.

The experimental test verifies the information of the datasheet, as the relation is lineal and is centered in 2.5 V. Next, the stalling experiment is made.
It is relevant to mention that two different tools are used. The first one is a click torque wrench. These kinds of tools work by predefining the torque to be applied. They do not have any kind of visual display or gauge, only a click when the applied torque reaches the setpoint. Naturally, this has a major drawback, as the current lecture needs to be measured at the same time that the click sounds, causing imprecisions. The available wrench can measure from 5 to 15 Nm.

The other tool is a dynamometer, which can measure from -3 to 3 Nm. It has a gauge that instantly returns the value of the torque measured. Even though it can be more precise, it is not the ground truth either.
The results are the following:

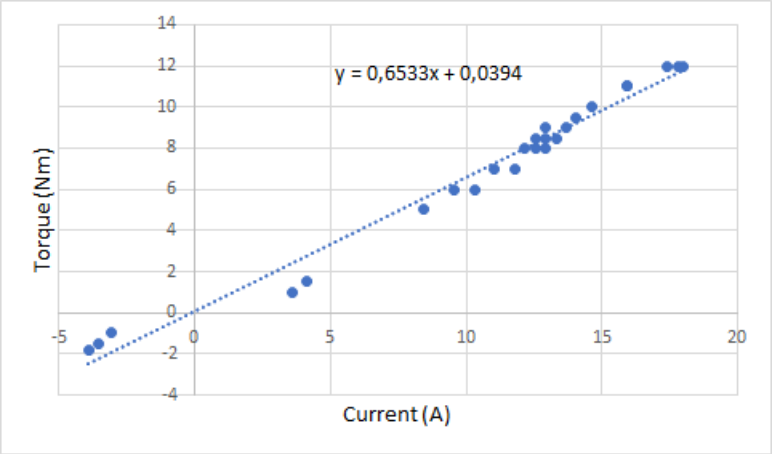


**Figure 6.10.** Torque-Current Relation.

As it can be seen, the result is far from being perfectly linear, but an approximation can be made. Inaccuracies can arise from the inherent low precision of the experiment, due to the tools used, and the design of the experiment itself. In any case, an approximation of $K_t = 0.653$ [Nm/A] is feasible.

## 6.4 Control hardware design

### 6.4.1 Computing unit

The computing unit is a critical part of the control loop since it must read the different sensors, execute the control algorithms, generate the physical control outputs, and communicate with the rest of the elements in the hierarchical pyramid of the car in a time-critical structure. As a result, the selected hardware must have enough computing capabilities to fulfill the design requirements.

Within the AD group, a dSPACE MicroAutoBox II is available for use, which is a real-time prototyping system designed for vehicle applications. It includes a 900 MHz processor, a wide range of digital and analog input/outputs, communications capabilities like CAN or Ethernet, and it's certified for automotive use. Furthermore, it can be easily programmed using Simulink and the C code generator, and provides an interface for the PC, which allows the online visualization of different variables.

From the mechanical point of view, the connectors are mechanically secured trough positive locking. Even though it is not small (200 x 225 x 50 mm), it can be accommodated in the vehicle, and the overall advantages make it the ideal computing unit for this application.


**Figure 6.11.** dSPACE MicroAutoBox II

### 6.4.2 Motor controller

A motor controller is needed to transform the control signals into power ones. There are various types depending on the kind of motor used, but H-Bridges are the simplest and most used among DC Motors. Mainly, they are composed by two pairs of electronic switches, such as transistors or IGBTs, which change the polarity of the voltage supplied to the motor depending on whether they are switched on or not. The most basic H-Bridge electronic circuit is shown as follows:

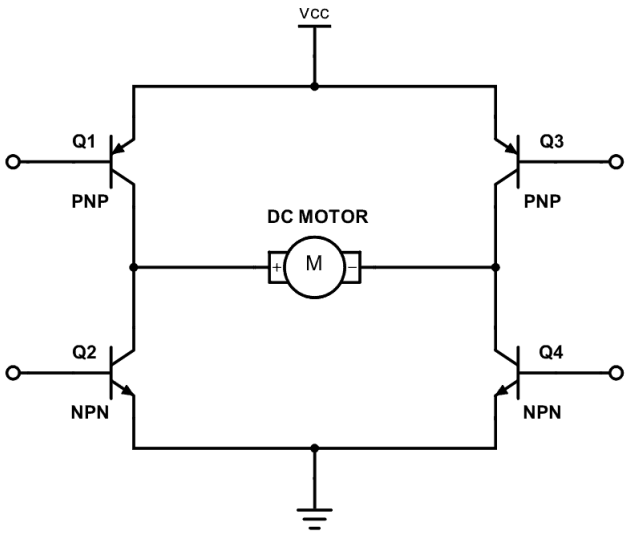


**Figure 6.12.** Electronic Circuit of an H-Bridge

When Q1 and Q4 are switched, the motor sees a positive voltage, whereas when Q2 and Q3 are switched, a negative voltage is seen by the motor. This allows driving the motor in both directions. Besides, the average voltage supplied to the motor depends on the duty cycle of the switches. In other words, driving the switches with a Pulse Width Modulation (PWM) allows the motor to rotate in a non-full speed operation.

Although the basics of H-Bridges are quite simple, motor drivers which control the switching are needed to avoid "shoot-throughs", which occur when two transistors of the same column are switched at the same time (i.e Q1 and Q2), even when it's only for a very little time. The electronic design and implementation of this circuit escapes the scope of the project, so a commercial device is used.

At first, an MDDS30 of Cytron Technologies is selected. This device is capable of driving motors up to 30 A continuously with a supply voltage from 7 to 35 V. Regarding the input, it can be sent as an analog or PWM signal. Nevertheless, some issues with the device were found during the development regarding the output change rate and the deadband around zero, which caused the change to a different commercial device.

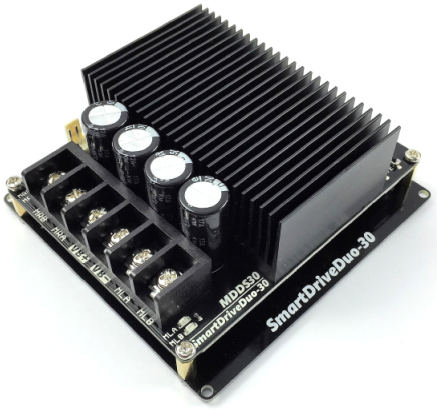


**Figure 6.13.** Cytron MDDS30 H-Bridge

This new H-Bridge, the Sabertooth 2x60, is capable not only of generating an output signal for an input signal as low as 0.01 %, but also allows complete customization of the slew rate of the output signal, including the generation of actual output steps. Furthermore, it is capable of withstanding up to 60 A continuously.

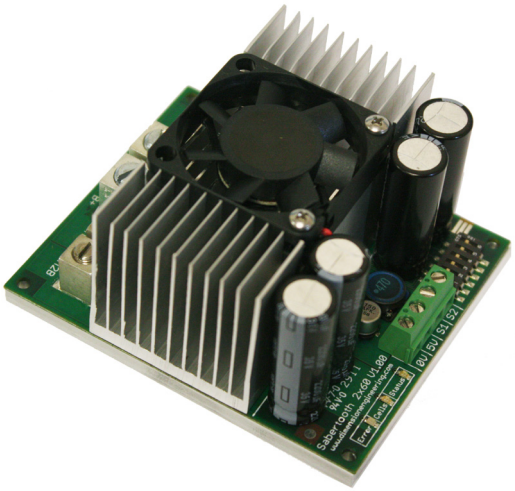

**Figure 6.14.** Sabertooth 2x60

### 6.4.3 PCB design

The hardware packaging is also a relevant aspect of the solution. During the early stages of the design, the mentioned sensors and conditioning circuits were placed in a protoboard, which offered high flexibility to modify and adapt the electronics. Nevertheless, to achieve a robust system capable of being mounted in a car and, therefore, withstand vibrations that could potentially loosen wires or disconnect sensors, a Printed Circuit Board (PCB) is needed.

Consequently, a simple 2-layer PCB consisting of the current sensor, the conditioning circuits and appropriate connectors is designed using Altium Designer.

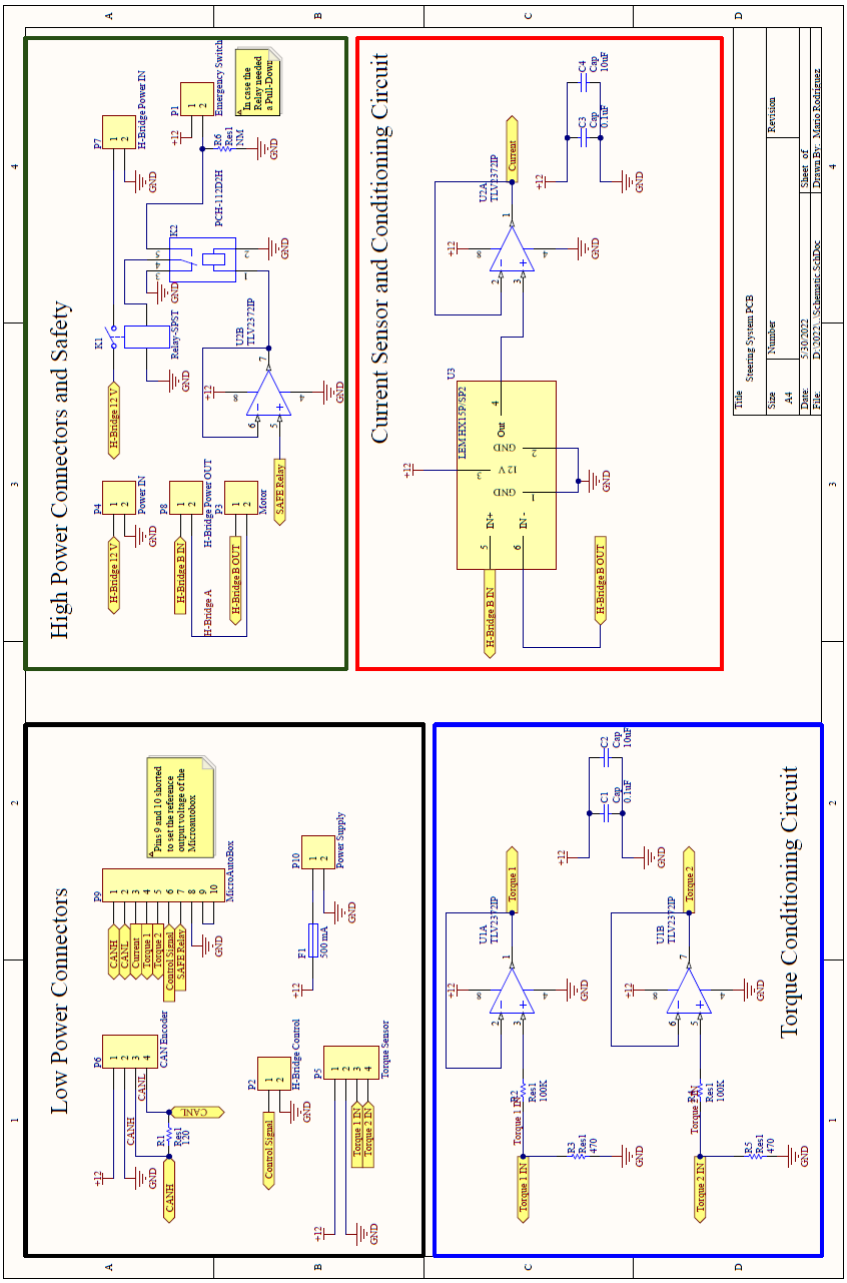


**Figure 6.15.** PCB Schematic

The PCB is also used to distribute power. Thus, the battery is connected to the steering system through the PCB. In the same way, the H-Bridge is powered through the PCB, and its output returns before reaching the motor. This way, the current flow can be measured in-board.

In addition to the strictly needed in the control system, safety-related components are added to the design. This includes fuses and a pair of cascade relays, which have the capabilities to disconnect the motor power supply. The actuation is made through an emergency switch and software.

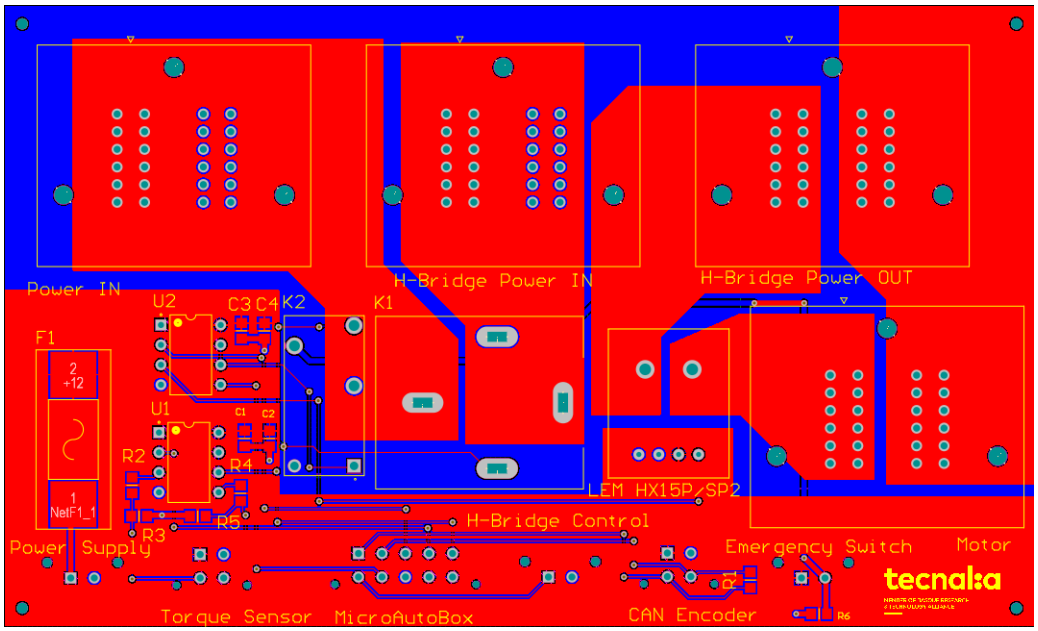


**Figure 6.16.** Components layout on the PCB

The layout in Figure 6.16 is distributed depending on the current flow. Thus, the upper part is reserved for high-current connectors, whereas the lower part is used for electronics. Furthermore, an appropriate flowing path for the high-current connections is ensured through the use of power planes.

## 6.5 System identification

After the initial description of the assembly, the following step is to obtain a dynamic model of the motor which allows the development of the control in simulation. A brushed DC motor is an electromechanical system whose mathematical model can be assimilated, in an ideal steady-state, with the following equations:

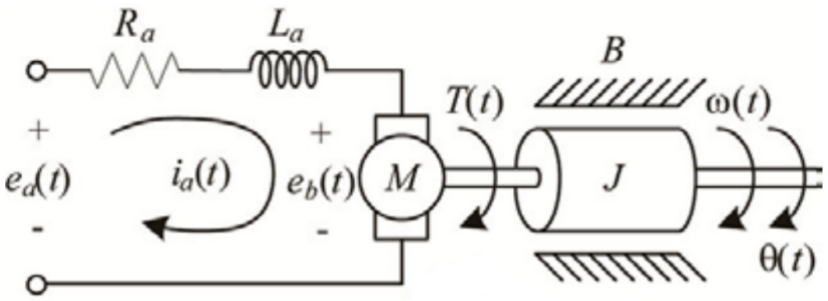


**Figure 6.17.** Physical structure of a DC Motor

Back electromotive force:

$$e_b(t) = K_E \cdot \omega_m(t) \qquad [V] \tag{6.2}$$

where $e_b$ corresponds to the back electromotive force, $K_E$ to the back electromotive force constant and $\omega_m$ to the shaft speed in rad/s.

Applying the Kirchhoff's voltage law to the armature circuit:

$$e_a(t) = R_a i_a(t) + L_a \dot{i_a}(t) + e_b(t) \qquad [V] \tag{6.3}$$

Developed torque:

$$\tau(t) = K_T \cdot i_a(t) \qquad [Nm] \tag{6.4}$$

where $\tau$ corresponds to the motor torque, $K_T$ to the torque constant, and $i_a$ to the armature current.

Mechanical torque:

$$\tau(t) = J\dot{\omega_m}(t) + B_m\omega_m(t) \qquad [Nm] \tag{6.5}$$

where $J$ is the motor rotational inertia and $B$ the damping coefficient.

In SI units, $K_E$ and $K_T$ are numerically equal. Thus, both are usually renamed as $K_M$. Combining the equations [6.2-6.5] and applying Laplace's transform, the

following transfer function which relates the motor speed to the applied voltage is obtained.

$$\frac{\omega_m(s)}{E_a(s)} = \frac{K_M}{(L_a J_m)s^2 + (L_a B_m + R_a J_m)s + K_M^2 + R_a B_m} \tag{6.6}$$

The position is obtained by multiplying 6.6 by 1/s. Thus, integrating in time.

If a speed reducer is used, being the motor shaft coupled to a gear with $N_1$ teeth and the load to a gear with $N_2$ teeth, with $N_1 < N_2$, the shaft speed decreases by $N_1/N_2$ whilst the torque increases by $N_2/N_1$.

$$\omega_L = \frac{N_1}{N_2} \cdot \omega_m \qquad [rad/s] \tag{6.7}$$

$$T_L = \frac{N_2}{N_1} \cdot T_m \qquad [Nm] \tag{6.8}$$

As a result, the transfer function that relates the load position with the voltage applied when the motor includes a speed reducer remains as follows:

$$\frac{\theta_m(s)}{E_a(s)} = \frac{K_M \cdot \frac{N_1}{N_2}}{(L_a J_m)s^3 + (L_a B_m + R_a J_m)s^2 + (K_M^2 + R_a B_m) \cdot s} \tag{6.9}$$

Due to the motor being disassembled, it is possible to check whether a speed reducer is present or not. Indeed, a speed reducer with a 13.5/1 ratio is used, meaning that the motor needs to spin 13.5 times for each spin of the output shaft.

First, experiments were carried out to identify the model transfer function as shown in equation 6.9. Two different approaches were considered. The first one consists of a parametric identification, which allows a better understanding of the model since every parameter has a physical meaning. On the other hand, a grey box identification with little physical meaning is also possible.

### 6.5.1 Parametric identification

In the beginning, efforts were focused on developing a parametric model. From the five available parameters ($R_a, L_a, K_m, J_m$ and $B_m$), the motor resistance and the inductance were measured with a multimeter. In Figure 6.10, the $K_M$ was calculated, but due to the inherent inaccuracies of the methodology used, it was used only as a starting point. It was then intended to adjust the remaining parameters.

One of the Matlab's Parameter Estimator examples [95] was used as a base model. In this example, a DC Servo Motor electromechanical model is implemented using

Simscape, being the parameters estimated with the Parameter Estimator Toolbox. The estimation required data from the motor response against different input waveforms, with the aim of using one for the estimation and a different experiment for validating the model.

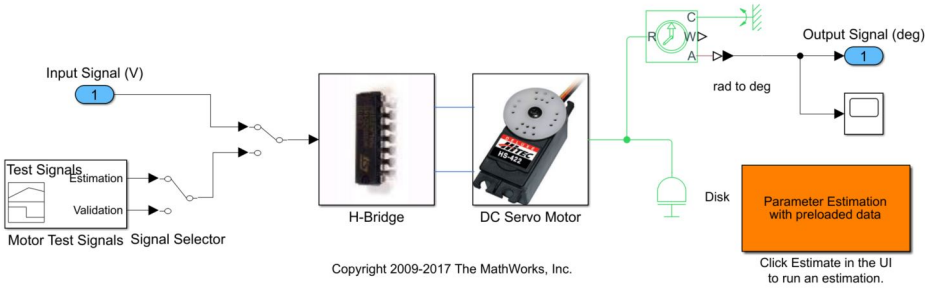


**Figure 6.18.** Simulink Motor Parameter Estimator [95]

To carry out the identification, a pair of experiments in which different square waves were supplied to the motor were made and recorded. In these experiments, shown in 6.19, the input was normalized between [-1 , 1], and the output motor position was measured with the shaft encoder, meaning that the speed reducer was included. The first experiment was used for the estimation itself, whereas the second one was used as validation data.

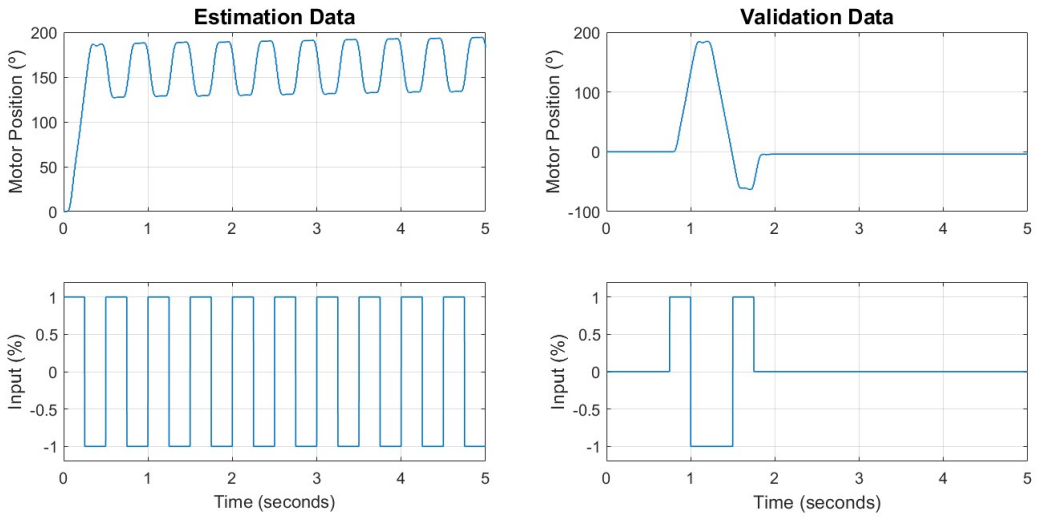


**(a)** Estimation Data **(b)** Validation Data

**Figure 6.19.** Experiments used for the parametric model identification

Several optimization methods, such as gradient descent, nonlinear least squares, and algorithms like Sequential Quadratic Programming, Trust-Region-Reflective were tested. The best result was obtained with a gradient descent method using a Sequential Quadratic Programming algorithm, which estimated the following parameters:

**Table 6.2.** Estimated Model Parameters

| $B_M$ [Nm · s/rad] | $J_M$ [Kg · s/rad] | $K_M$ [Nm/A] | $L_a$ [mH] | $R_a$ [Ω] |
|---|---|---|---|---|
| $3.1 \cdot 10^{-3}$ | $8.67 \cdot 10^{-5}$ | 0.04 | 0.146 | 1.9 |

The model response against both the estimation and validation data is now presented:

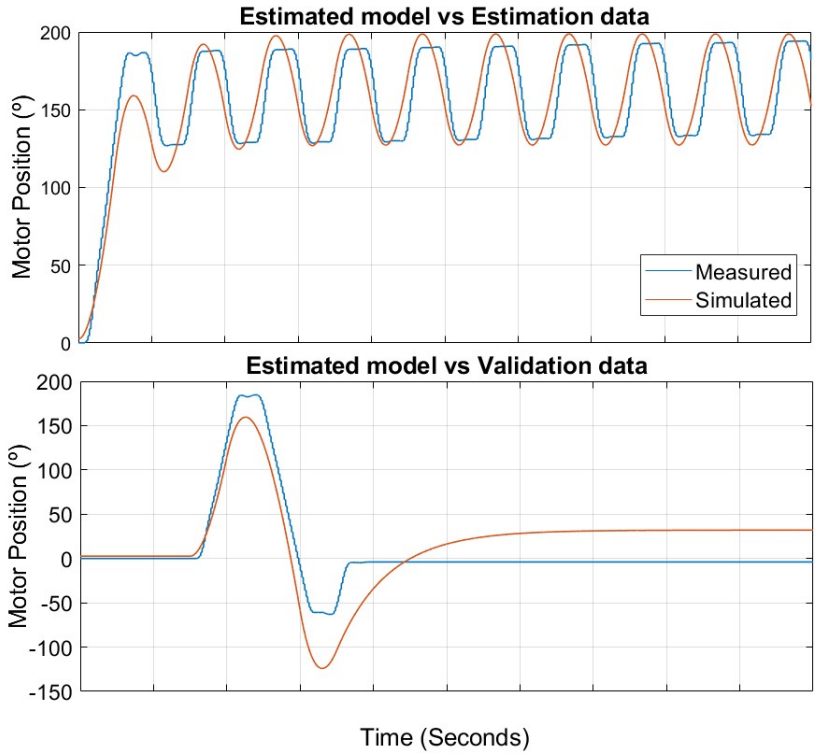


**Figure 6.20.** Parametric model comparison against estimation and validation data

The estimated model presented an indeed good correlation with the estimated data used for the parameter optimization, except for the initial transitory. Nevertheless, differences were more notorious when the model was simulated with the validation input data. Besides, the $K_M$ constant calculated by the optimization process in 6.2 and the experimentally calculated in the Figure 6.10 differ by order of magnitude, questioning the accuracy of the model.

The experiment was then repeated but, instead of the experiments shown in Figure 6.19, a new pair of measurements were recorded and used. The input signals were a pair of widely-separated steps for the estimation data, whereas a sinusoidal waveform signal was used for the validation data.

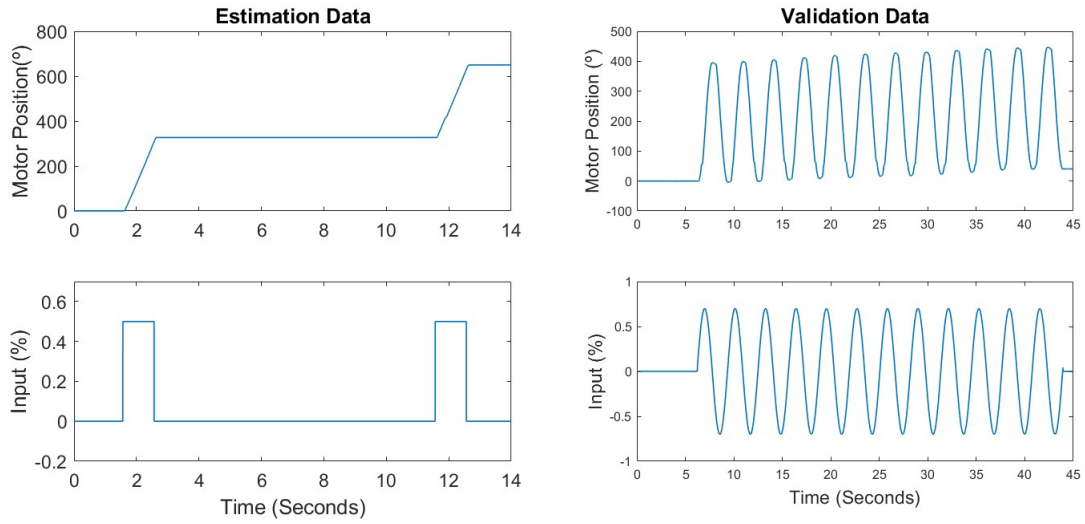


**(a)** Estimation Data **(b)** Validation Data

**Figure 6.21.** Experiments used for the second identification

The optimization methods were the same as in the previous experiment, but this time the best result was obtained with the Nonlinear Least Squares using a Trust-Region-Reflective algorithm. The parametric values obtained were the following:

**Table 6.3.** Estimated Model Parameters in second experiment

| $B_M$ [Nm · s/rad] | $J_M$ [Kg · s/rad] | $K_M$ [Nm/A] | $L_a$ [mH] | $R_a$ [Ω] |
|---|---|---|---|---|
| $1.18 \cdot 10^{-2}$ | $3.5 \cdot 10^{-8}$ | 0.032 | 0.04 | 1.9 |

The simulation presented the same pattern as in the first identification attempt. Whereas the response of the estimated model is almost perfectly fitted, the validation data presents notable differences that discourage the use of the model for further developments.

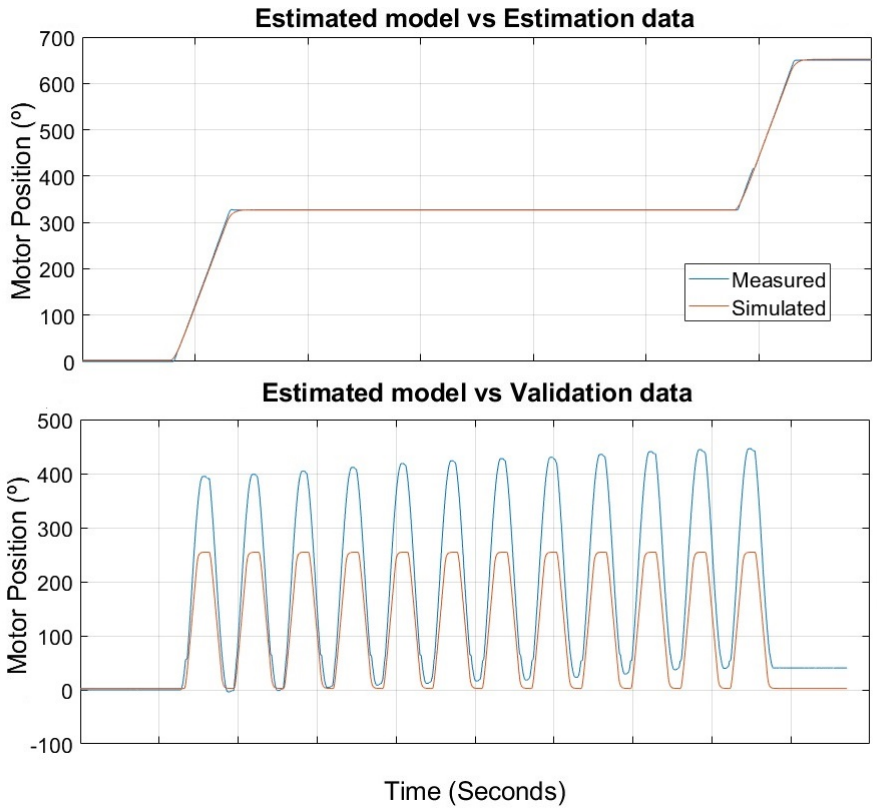


**Figure 6.22.** Parametric model comparison against estimation and validation data in second experiment

### 6.5.2 Grey-box identification

Since the optimization process was clearly not good enough, a different approach was required. This time, the aim was to estimate a grey-box model, which means that the poles and zeros structure is known and defined, but the coefficients are to be determined. As a result, a third-order transfer function with the structure of 6.9 that best suits the dynamics of the motor was looked for. As previously said, the grey-box optimization loses the physical meaning of the parameters but is more flexible in terms of non-considered non-idealities of the mathematical model.

The model estimation was also carried out in Matlab, using the System Identification Toolbox. This Toolbox is capable of running estimations searching for transfer functions with user-defined poles and zeros structure with different optimization algorithms as needed.

The experiments used for the identification were the ones presented in Figure 6.21, thus, the ones used for the second identification attempt.

Once again, the Toolbox allows using different search methods to execute the estimation, such as Gauss-Newton, Levenberg-Marquardt, gradient descent, Trust-

Region Reflective Newton or Sequential Quadratic Programming. Besides, stability is one of the configuration parameters that can be enforced.

The Gauss-Newton method obtained the best result, achieving a 99.26 % fit to estimation data and an 83.99 % to the validation data while enforcing stability.

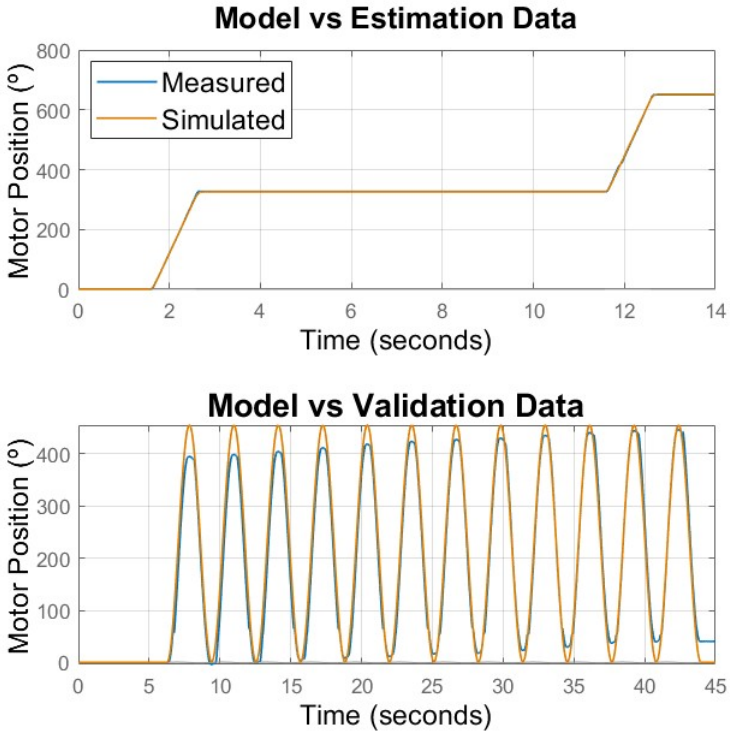


**Figure 6.23.** Grey-box model comparison against estimation and validation data

The resulting transfer function was the following:

$$\frac{\theta_m(s)}{E_a(s)} = \frac{5.367 \cdot 10^5}{s^3 + 55.47s^2 + 823s} \tag{6.10}$$

With the aim of calculating stability limits of the model, both Root Locus analysis and Bode diagram were calculated with a hypothetical proportional controller.

As it can be seen in 6.24, there is one pole at the origin, an integrator, and a pair of complex poles in the left semi plane. This means that the closed loop is stable as long as the controller gain stays below approximately 0.08. Thus, the Bode diagram is simulated in a closed loop with a gain of 0.01.

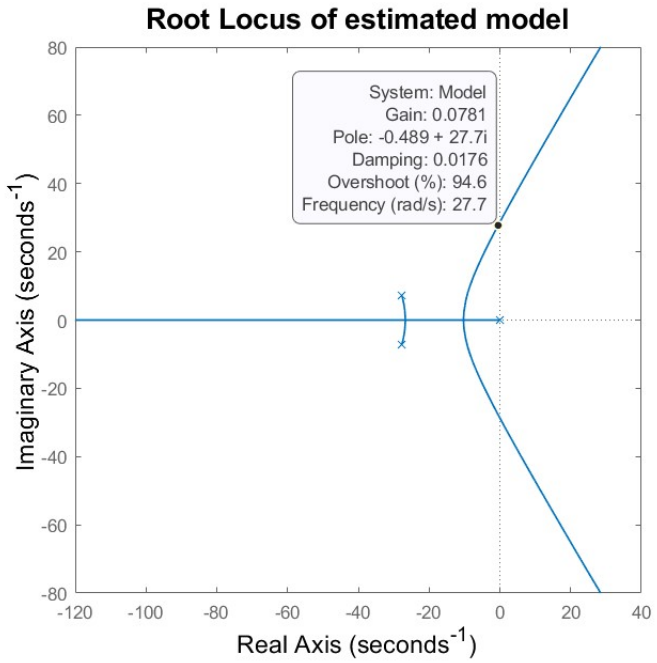


**Figure 6.24.** Root Locus of the estimated model

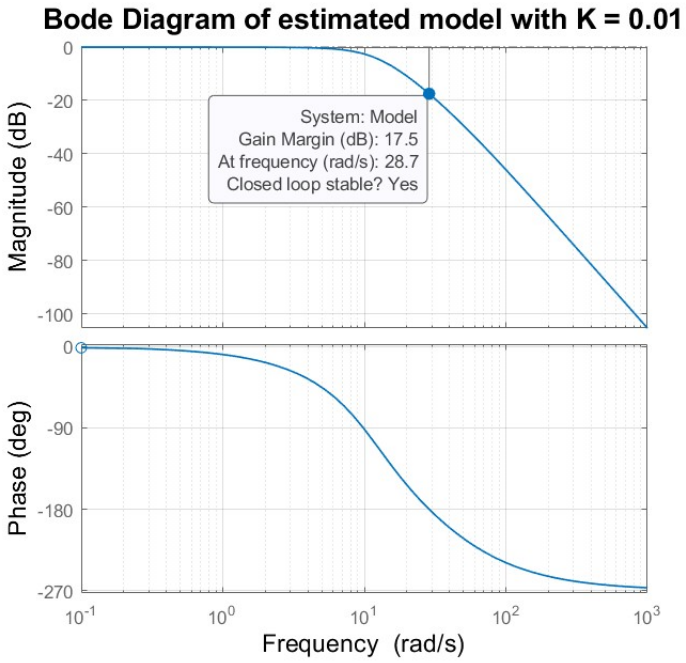


**Figure 6.25.** Bode diagram of the estimated model in closed loop with K = 0.01

The bode diagram shows a gain margin of 17.5 dB and an infinite phase margin. As a result, the stability with this range of gains is ensured even if there were model inaccuracies.

### 6.5.3 Discretization

So far, the model and analysis have been developed in continuous time, but the deployment target is a discrete-time controller, which means that the obtained transfer function needs to be discretized.
The discrete-time transfer function depends on the sample time, which leads to a problem. Whereas the available encoder works at a 10 ms rate, in section 6.2 was stated that the position control loop needs to run at a 1 ms rate, which corresponds to the rate of the encoder that is currently mounted on the car, and is unavailable.

As a result, it was decided to compute discretizations at both sample times and compare them.

Using Matlab to compute the 10 ms discretization with a zero-order hold retainer, the result is the following:

$$\frac{\theta_m(z)}{E_a(z)} = \frac{0.078z^2 + 0.272z + 0.0591}{z^3 - 2.515z^2 + 2.086z - 0.5742} \tag{6.11}$$

Repeating the same operation with a 1 ms sample time returns the following discrete transfer function:

$$\frac{\theta_m(z)}{E_a(z)} = \frac{8.822 \cdot 10^{-5}z^2 + 3.48 \cdot 10^{-3}z + 8.581 \cdot 10^{-5}}{z^3 - 2.945z^2 + 2.891z - 0.946} \tag{6.12}$$

A root locus analysis with a hypothetical P controller is now made on both discrete-time models, in order to obtain stability limits with both sample times:

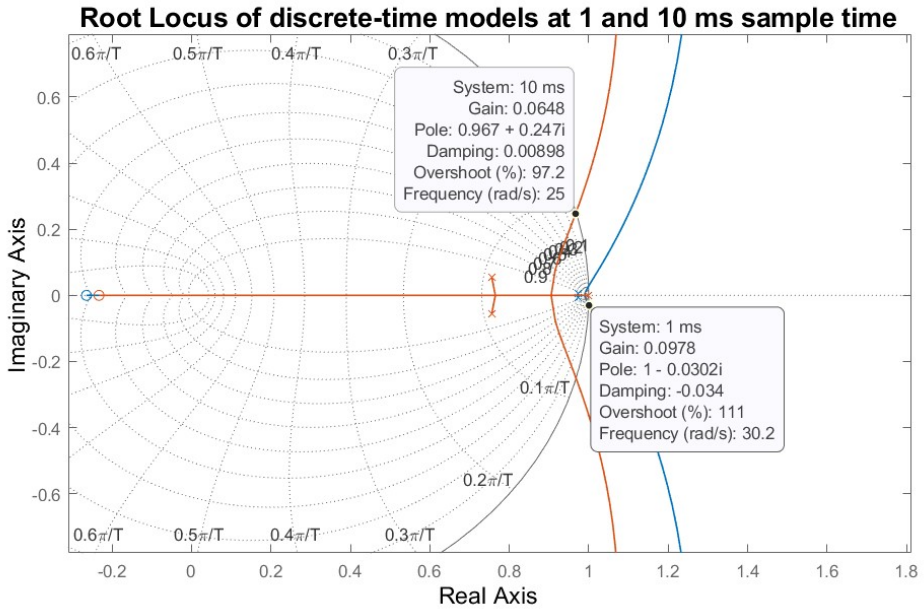


**Figure 6.26.** Root Locus of the discrete-time estimated models at 1 and 10 ms sample time

As Figure 6.26 shows, an approximately 0.07 gain, which corresponds to the limit of the unitary circle, establishes the stability limit when controlling at 10 ms. By contrast, the limit rises until 0.09 when the sample time descends to 1 ms, although the poles are closer to the circle limits. All gains below the mentioned lead to a stable closed-loop system.

## 6.6 Control

Once the motor is modelled, the control can start to be developed. As stated before, the project's primary goal is to substitute the current steering system of an automated Renault Twizy for a more powerful one suitable for shared control algorithms, which depend on torque control. However, the vehicle needs to continue being capable of performing use cases of fully automated driving. As a result, both a position and a torque control need to be designed.

### 6.6.1 Position control

Starting with the position control, both models obtained in equations 6.11 and 6.12 had a pair of complex poles inside the unitary circle and a pole at $1 + 0i$. Consequently, the plant already has an integrator, and closed-loop steady-state error against step inputs would be, theoretically, zero.

Therefore, a proportional controller in a closed-loop could be enough to ensure an appropriate reference tracking. As it was calculated in Figure 6.26, the gain needs to remain below 0.07 to guarantee stability.

A simulation with a gain of 0.015 is now presented. The input signal used is a composition of ramps which intend to replicate the operation point of the system in the car.

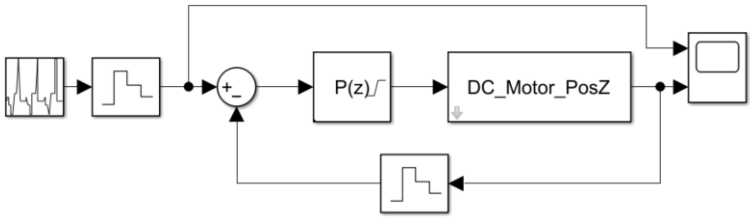


**Figure 6.27.** Control loop of position control

Figure 6.28 shows a reasonable good tracking performance, with very little overshoot, an indeed fast rise time and no steady-state error.

Once the control is successfully simulated, it is programmed in the MicroAutoBox. As said before, it is easily programmable in Simulink, which through C code generation, creates files that are deployed.

However, after the deployment, some differences between the model and the real-world operation of the system came to light. When the control signal was below 15 % in absolute value, the H-Bridge did not respond, causing a non-linearity in the system. This phenomenon appeared when the error was close to zero, avoiding the eliminating of the steady-state error and causing vibrations due to the overshoot

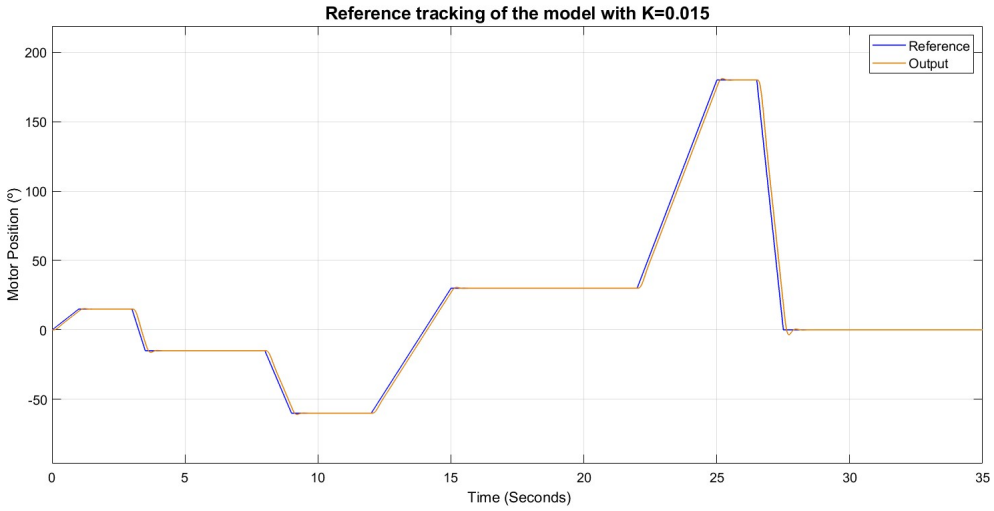


**Figure 6.28.** Position control simulation

caused by steering wheel inertia. As was anticipated in section 6.4.2, it was one of the factors that led to the decision to change the Cytron H-Bridge for a Sabertooth 2x60 H-Bridge.

Actual measurements with the improved H-Bridge and different proportional gains are now presented. The first two correspond to static gains of 0.015 and 0.03, respectively, whereas the remaining two are related to scheduled gains, which depend on the reference change rate and the instantaneous error. If the reference changes more than 0.15º in 10 ms or the error is bigger than 1.5º, the proportional gain equals 0.03 for the first controller and 0.05 for the second one. Otherwise, their values are, respectively, 0.015 and 0.03.

Figure 6.29 shows the tracking performance of the proportional controller on the existing system. All four controllers achieve a decent tracking capability, but the steady-state error remains with lower gains due to model inaccuracies. As can be seen, especially in the close-ups, the best performance is achieved by the 0.03 to 0.05 scheduled gain, which combines a smooth response when the reference suffers minor variations and the error is minimal with a more aggressive one when needed. As required in Table 6.1, the steady-state error remains below 1.5º.

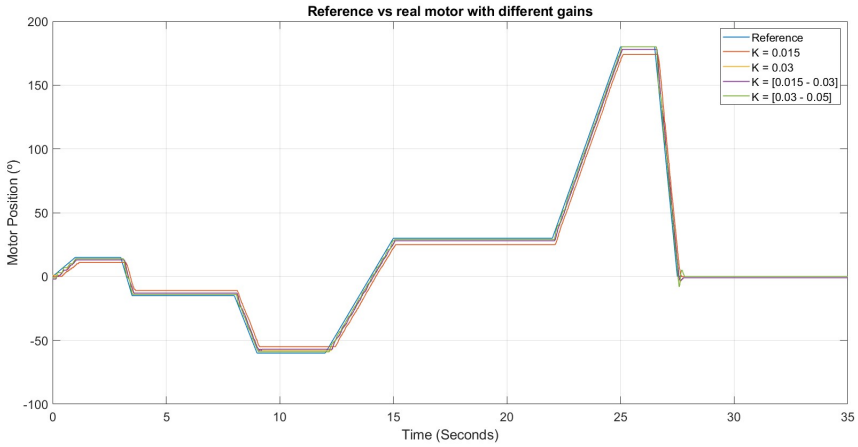


**(a)** Reference vs output measures with different gains

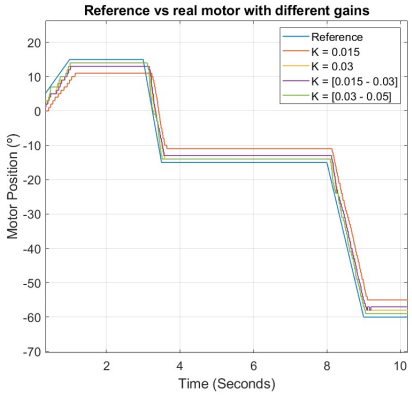


**(b)** Close up

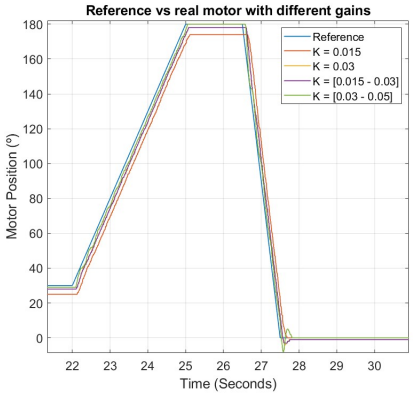


**(c)** Close up

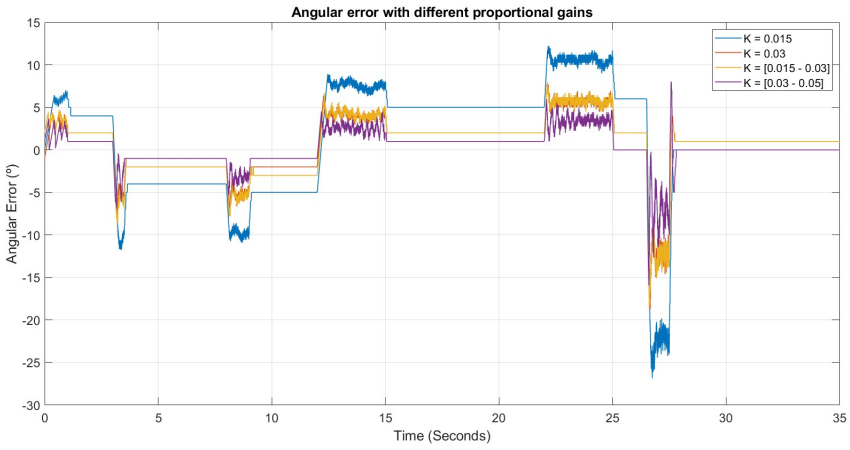


**(d)** Angular error

**Figure 6.29.** Reference and output measurement comparison with different gains

A comparison between the current position control with the scheduled gain and the model obtained in section 6.5 using the same computed gain are presented in Figure 6.30.

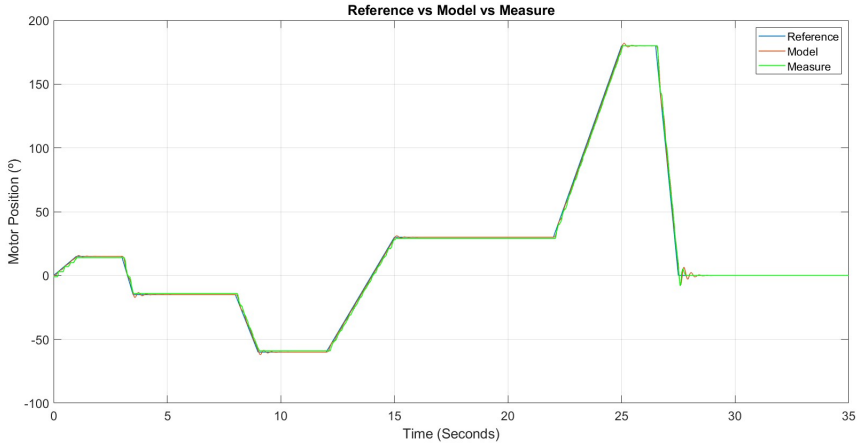


**(a)** Model vs output measurement

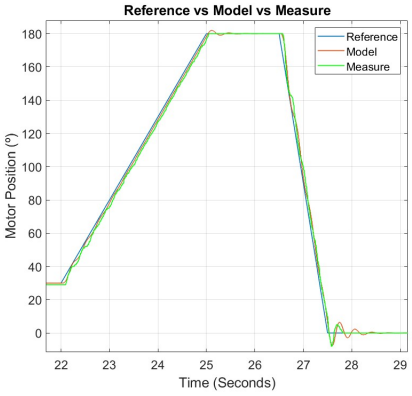


**(b)** Close up

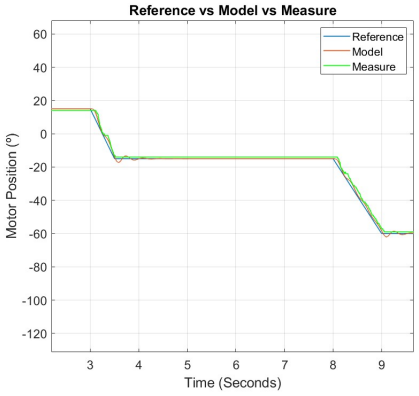


**(c)** Close up

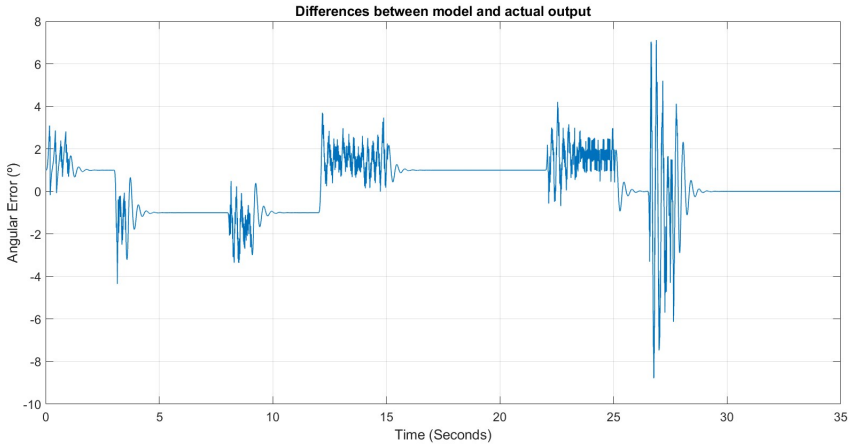


**(d)** Angular error between model and actual output

**Figure 6.30.** Model and output measurement comparison with scheduled gain

Figure 6.30 shows an indeed good correlation between the computed discrete-time model and the current motor, being the differences between them almost always below $\pm 3^o$. The estimated model is, however, less damped in terms of transitional response. Nevertheless, it is overall a good model.

Finally, subsequent tests are done with the aim of corroborating the controller's robustness against different mechanical frictions that can be applied when operating on the road in the actual car. With the intention of simulating this effect, a pair of adjustable felt clamps are installed on the steering column.

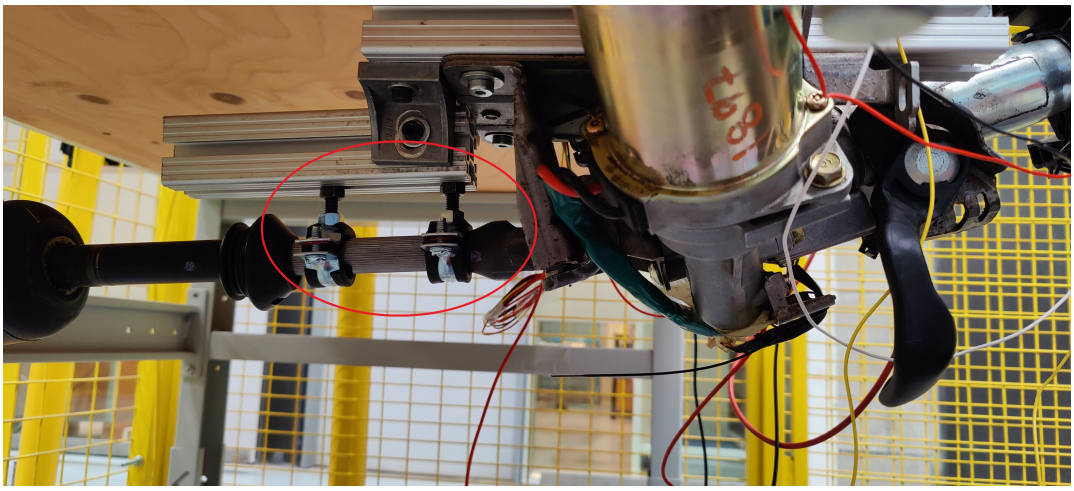

**Figure 6.31.** Adjustable felt clamps

The obtained results are the following:

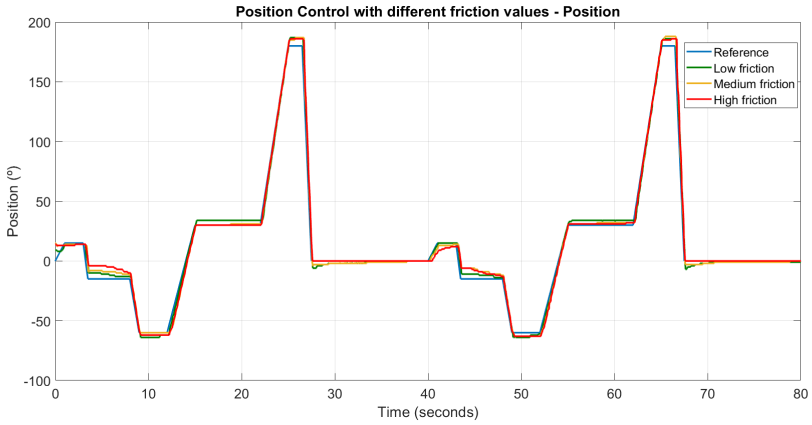


(a) Position Comparison

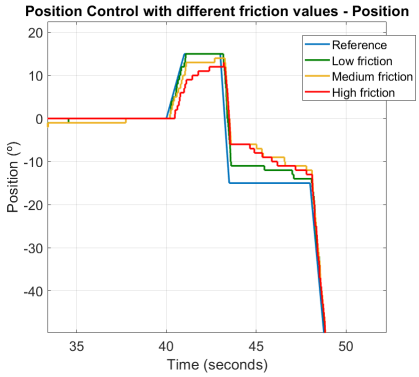


(b) Close up

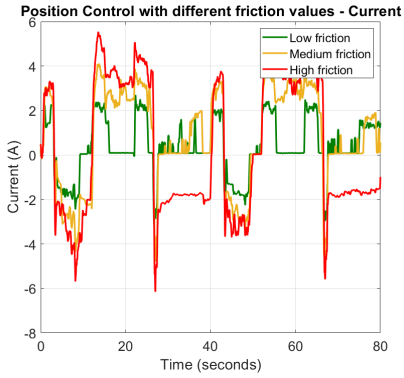


(c) Current comparison

**Figure 6.32.** Comparison between different friction values

As shown in Figure 6.32, the tracking performance is obviously decreased, being the system slower, but an appropriate steady-state is nonetheless achieved. The current consumed is higher the more friction is present, as could be imagined. The tire's friction is one of the most varying parameters of the car, depending on the surface type and whether it is wet or not. Thus, it was opted to remain using a proportional controller instead of using a PI and, consequently, adding another pole in origin.

In conclusion, a controller has been designed keeping in mind the idea of maintaining it as simple as possible without neglecting an adequate performance according to the design requirements, which has resulted in being a proportional controller due to the inherent integrator in the plant. Furthermore, the gain has been kept low enough to avoid instabilities and undesired behaviours when mounting the steering system with the faster encoder, thus, decreasing the control loop's time rate to 1 ms.

### 6.6.2 Torque control

Both humans and automated systems cooperate in the driving task in shared control. The effectiveness and acceptance of shared control algorithms for automated driving highly depend on the driver's feelings with, in this case, the steering wheel. Humans are used to drive applying torque, which is needed to overcome the natural self-aligning torque produced by the tires as they roll along, which tends to steer the vehicle to a straight position. Thus, the low-level control needed for these algorithms has torque as the controlled variable.

As was shown in equation 6.4, the developed torque by the motor is directly proportional to the armature current, but the mechanical torque which is applied to the steering shaft also depends on the inertia and damping of the system. As it was, on the one side, not possible to obtain a reliable parametric model of the motor, and on the other side, those values were to change when the motor assembly was installed on the car, where modelling is unfeasible due to mechanical restrictions, it was decided not to obtain a mathematical model which relates voltage to torque. Altogether, the controller tuning needed to be done without prior knowledge of the system dynamics.

Motor torque, the controlled value, is obtained by multiplying the calculated $K_T$ of the motor by the current sensor measurement. As is evident, the quality of the control depends on a clean sensor signal. Due to the natural characteristics of the measured signal, it is indeed very noisy. Part of the noise could be blamed on disturbances affecting the sensor, but the truth is that the vast majority of high-frequency components of the measured signal are caused by the H-Bridge switching. With a PWM frequency of 24 kHz, the continuous change between +12 and -12 V generates a high-frequency current ripple, which is measured by the sensor. As a result, the measurement is heavily distorted.

With the intention of cleaning the signal, a set of experimentally tested filters is applied to the current measurement. A moving average with a 10 sample window, followed by a second decimal rounding, a Kalman filter and a rate of change limiter, is applied to the actual measurement. As a result, the signal used in the control loop is much smoother.

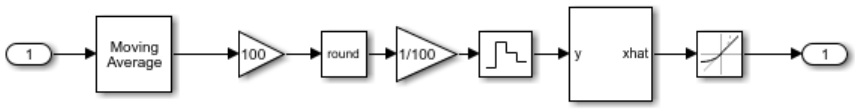


**Figure 6.33.** Set of filters used

Despite the evident benefits of filtering the signal, there are also counterparts. As the filtering needs to be done online, a delay between the real value and the filtered

one is also added. The key to an appropriate control resides in the balance between these two mentioned effects.

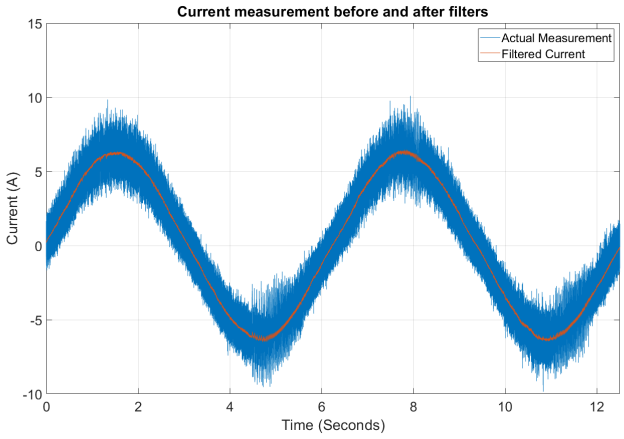


**Figure 6.34.** Actual current measurement vs filtered signal

As can be seen in Figure 6.34, a great improvement is achieved. Even though the filtered current is much smoother and cleaner than the actual one, there is some remaining high-frequency component. Trying to minimize this led to excessive delays compared to the original measurement.

Controlling the motor by torque means that a resistant torque needs to be applied to the steering wheel. Otherwise, it would spin freely at maximum speed, and yet the torque reference would not be reached. Consequently, all graphics shown in this section were recorded handling the steering wheel and applying resistant torque, which translates into disturbances.

The designed control loop is based on a PI controller and was first tested on a simplified self-aligning torque simulation. This application generates a torque reference proportional to the angle of the steering wheel and with a sign change, so the steering wheel always tends to align in the centre, executing more torque the more deviated it is.

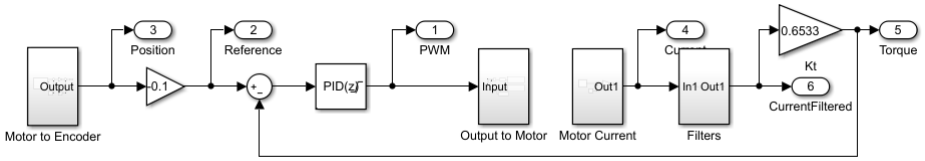


**Figure 6.35.** Torque Control Loop

Due to the temporal execution of the project, the first iterations of the control were made with the Cytron H-Bridge, whose limitations became visible once again. As Figure 6.36 shows, huge vibrations were produced when the control signal average was below 0.2 %.

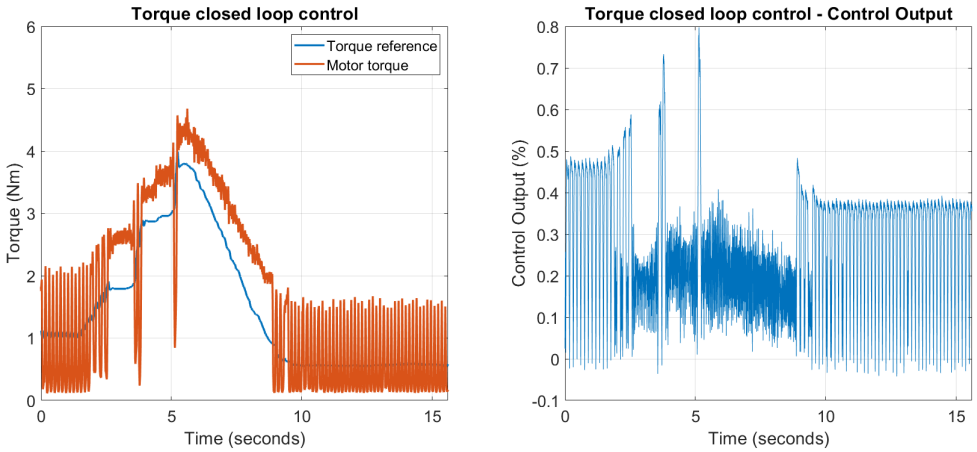


**(a)** Torque output. Self-Aligning Torque

**(b)** Control signal. Self-Aligning Torque

**Figure 6.36.** Torque output and control signal with Cytron H-Bridge. Self Aligning Torque simulation

The cause was a non-programmable deadband implemented in the H-Bridge. When the control signal fell below this threshold, the output voltage generated by the H-Bridge was zero, meaning that the current also dropped to zero and, therefore, the torque. As a result, the error would rise, rising almost instantaneously the control signal. The repeat of this loop caused the vibrations.

Several experimental strategies were unsuccessfully tried with the intention of minimizing the aforementioned effect. Among these were included bi-dimensional lookup tables that modified the control signal depending on the error, dynamic rate of change of the control signal limiters or gain scheduled PI controllers, but none of them was successful.

Open-loop control was also tried, which even outperformed the closed-loop in terms of vibrations. However, as can be imagined, it entailed an inferior tracking performance, as Figure 6.37 shows.

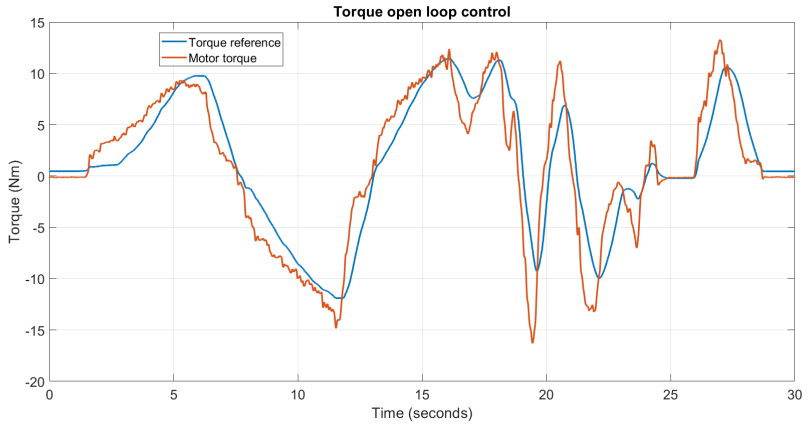


**Figure 6.37.** Torque Control Open Loop. Self Aligning Torque simulation

The unsatisfactory performance with either option was another of the significant drawbacks that led to the change of H-Bridge. Similar tests were conducted with this new device in closed-loop control with a PI controller. The achieved results are the following:

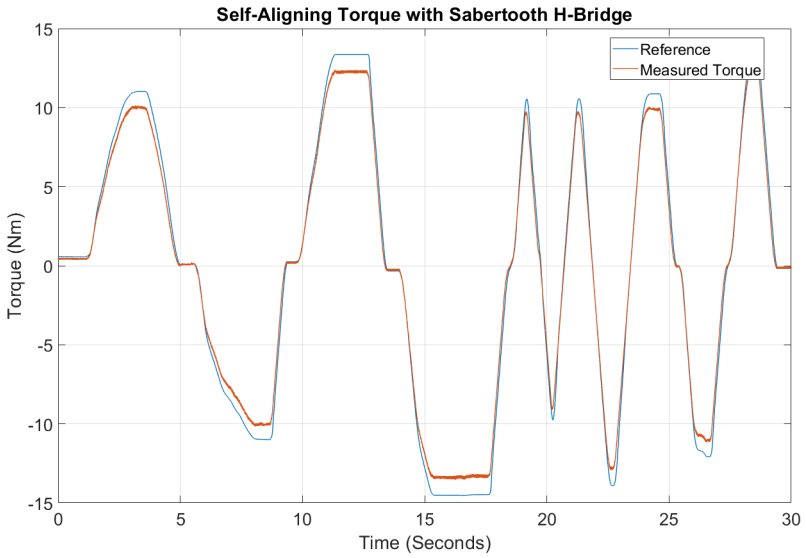


**Figure 6.38.** Self Aligning Torque simulation with Sabertooth H-Bridge

The tracking performance with the Sabertooth displayed in Figure 6.38 is much higher than the one that the Cytron could offer due to its output linearity capabilities. Nevertheless, difficulties in reaching the reference when it surpasses approximately 10 Nm are evidenced, but the design requirement of exerting at least 10 Nm is reached.

Further tests were carried out on the torque control, but a predefined waveform reference was applied instead of the self-aligning torque application. After testing several controller parameters, the following three shown in Table 6.4 achieved the best performance. Due to the noise localized even in the filtered current in Figure 6.34, controllers including derivative action showed worse performance than the ones only including proportional and integral action, whereas pure proportional controllers did not achieve an adequate tracking performance.

**Table 6.4.** Controller parameters tested

| | P | I |
|---|---|---|
| Controller 1 | 0.2 | 0.05 |
| Controller 2 | 0.5 | 0.05 |
| Controller 3 | 0.3 | 0.08 |

The experiments had the following result:

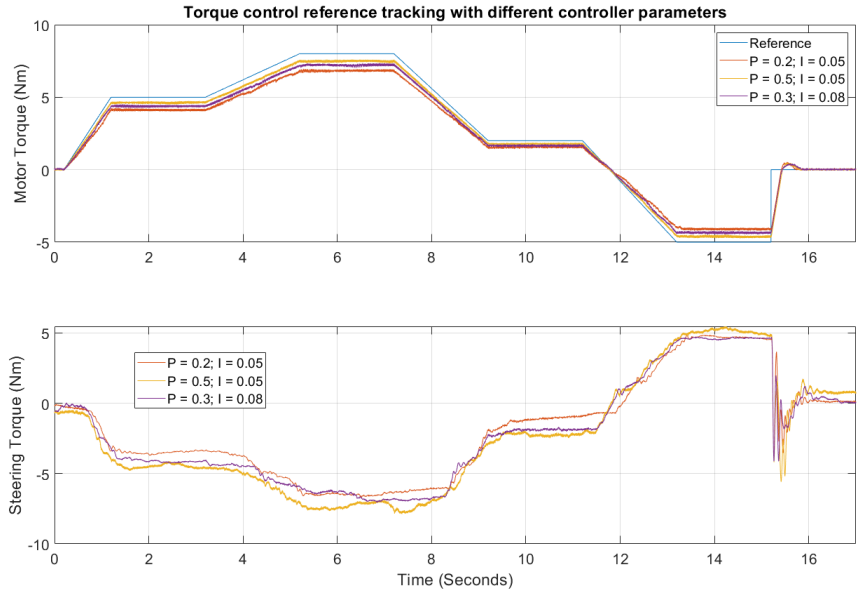


**(a)** Reference tracking and steering torque

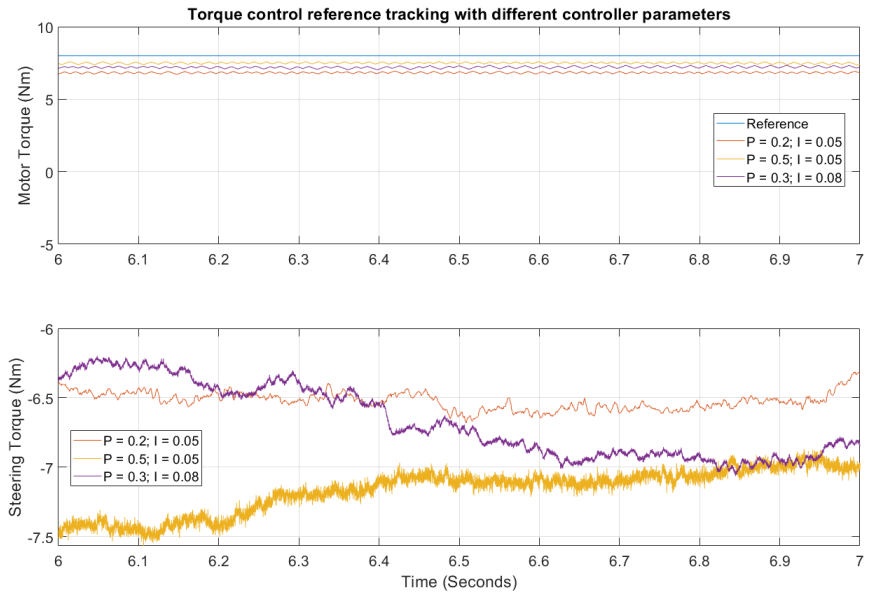


**(b)** Close-up

**Figure 6.39.** Motor torque reference tracking and measured torque at the steering wheel

Some relevant conclusions can be extracted from Figure 6.39. On the one hand, the tracking performance is better the higher the proportional gain, but the steady-state error is not eliminated. Besides, some overshoot can be appreciated under step changes in the reference for all three controllers.

On the other hand, the lower part of each Figure displays the mechanical torque applied to the steering wheel. The rotational direction of the motor and handling

torque have opposite signs but almost equal absolute values. Nevertheless, what is truly relevant is the coupled noise to the signals. As Figure 6.34 showed, the current signal used to compute the error in the control loop cannot be perfectly filtered. Thus, the error signal inherits the ripple, which is then amplified and sent back to the motor by the proportional action of the controller. As a result, a high-frequency vibration can be felt when handling the steering wheel and measured by the torque sensor.

In shared control, nice and smooth handling is as relevant as a good tracking performance. When improving one of them affects negatively the other, a middle ground must be reached. As can be seen, the ripple with the controller with the highest proportional gain is significantly higher than the other two, being the tracking performance only slightly better. However, lowering the proportional and rising the integral part allowed to balance both objectives, following the reference with the best possible accuracy, whilst producing a smooth feeling when handling. As a result, it was decided to implement controller 3 of Table 6.4, which fulfils the steady-state error requirement of Table 6.1 ($e_{ss} \leq 1$ Nm) and suffers low ripple.

## 6.7 Validation tests - Dynacar

The performance of the torque controller with more realistic steering profiles was evaluated using Dynacar, a Real-Time vehicle dynamics simulation environment developed within Tecnalia Research & Innovation [96].

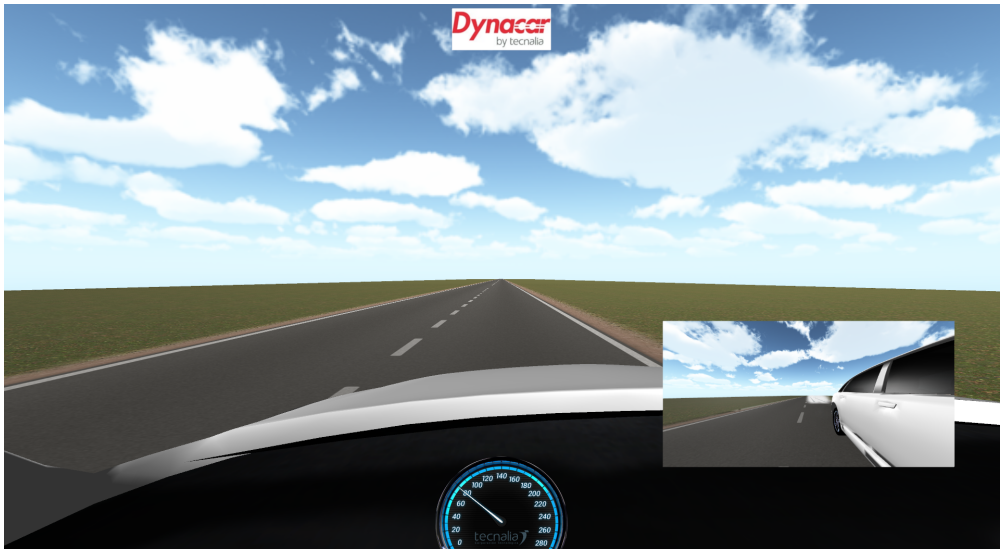


**Figure 6.40.** Dynacar vehicle dynamics simulator [96]

The followed procedure was as follows: First, a shared control algorithm developed within the research group was selected. Then, the AUDRIC [55] framework for MATLAB/Simulink was adapted to accommodate the developed solution. As explained before, the solution focuses on the Actuation module of the architecture, which needed to be modified to receive the motor information through CAN. Next, the MPC weights of the high-level control needed to be slightly tuned to achieve a satisfying overall response, since the motor position, torque and the steering wheel torque are taken as inputs in the high-level control. Finally, the controller was tested.

The experiment lasted about forty seconds, from which the first twenty were used to test the behaviour under normal circumstances. Hence, soft torques simulating driver distractions were applied to the steering wheel, aiming to deviate the car from the lane. Then, the controller was pushed to the limits, and a strong swerve was applied, with the intention of testing the response in emergency cases. The achieved results are the following:

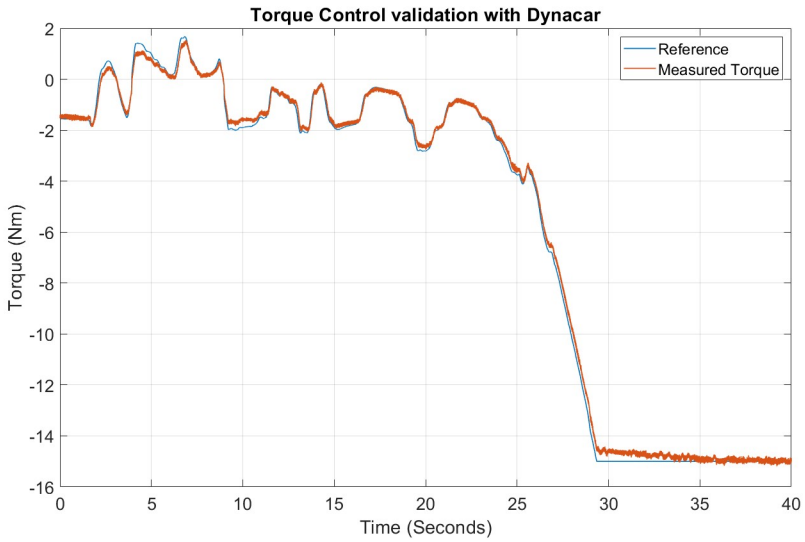


**(a)** Reference vs motor torque

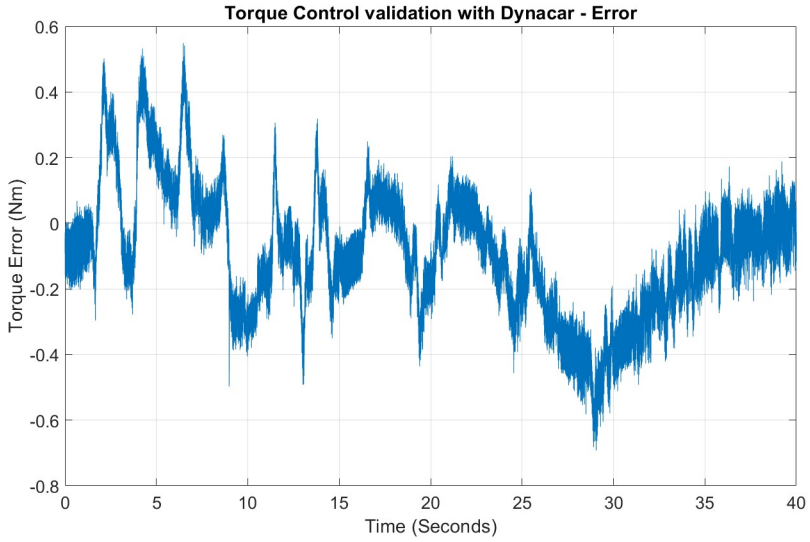


**(b)** Torque error

**Figure 6.41.** Torque control validation with Dynacar

As Figure 6.41 displays, the controller achieves a good tracking performance during the entire experiment. The controller responds adequately when the reference changes moderately, even though its performance is reduced when the reference changes abruptly. Nonetheless, the controller does not produce overshoot, which benefits the feeling when handling the steering wheel, whereas the error is maintained below 0.6 Nm while producing a low ripple. This threshold error is only surpassed when the emergency manoeuvre is initiated, and the high-level controller saturates at 15 Nm, which is the maximum allowed torque due to security reasons. Overall, the developed controller is indeed appropriate for the application it was designed for.

## 6.8 Deployment

This section aims to cover the final considerations beyond the control algorithm that must be considered and implemented in the MicroAutoBox.

### 6.8.1 FMEA - Failure Mode and Effects Analysis

All systems involving medium or high currents and moving parts entail an inherent potential risk in case of failure. Besides, human lives could be endangered when it is part of an automotive application. A failure analysis based on the FMEA methodology is carried out to reduce these risks. This method covers the location of potential failures, their consequences, the detection method, and the handling sequence to prevent them from happening or mitigate their effect.

The following table is the result of the analysis:

**Table 6.5.** Failure Modes and Effects Analysis

| Item | Category | Failure | Consequences | Detection | Handling |
|---|---|---|---|---|---|
| Motor | Power Supply | Broken / disconnected wire | Motor doesn't move | Control output and encoder / current sensor check | Critical error |
| Motor | Power Supply | Wrong connection | Motor moves in the opposite direction | Control output and encoder / current sensor check | Critical error |
| Motor | Mechanical | Mechanical block | Motor doesn't move | Control output and encoder / current sensor check | Critical error |
| H-Bridge | Power Supply | Broken / disconnected wire | Motor doesn't move | Control output and encoder / current sensor check | Critical error |
| H-Bridge | Power Supply | Wrong connection | H-Bridge could be damaged | Control output and encoder / current sensor check | Critical error |
| H-Bridge | Communication | AN wire (% VCC) broken / short circuited to GND/VCC | Motor moves at full speed / doesn't move | Control output and encoder / current sensor check | Critical error |
| H-Bridge | Communication | GND wire broken / short circuited to VCC | Unexpected motor behavior | Control output and encoder / current sensor check | Critical error |

**Table 6.5.** Failure Modes and Effects Analysis

| Item | Category | Failure | Consequences | Detection | Handling |
|---|---|---|---|---|---|
| Controller | Power Supply | Broken / disconnected wire | Motor doesn't move | Periodic handshake with PLC | Critical error |
| Controller | Code failure | Bug in the code | Unexpected motor behavior | High-level supervision | Critical error |
| Controller | Communication | Faulty communication with PLC: Data Corruption | Position / Torque reference doesn't update | CAN error handling | Resettable error |
| Controller | Communication | Faulty communication with PLC: Loss and delay of messages | Position / Torque reference doesn't update | Transmission time outs | Resettable error |
| Controller | Communication | Faulty communication with encoder: Data Corruption | Position open loop | CAN error handling | Resettable error |
| Controller | Communication | Faulty communication with encoder: Loss and delay of messages | Position open loop | Transmission time outs | Resettable error |
| Controller | Wrong parameters | Control mode not available | Motor doesn't move | Data Missing in CAN package | Config. mode |
| Controller | Wrong parameters | Reference not available | Motor doesn't move | Data Missing in CAN package | Resettable error |
| Encoder | Power Supply | Broken / disconnected wire | Position open loop | Control output and encoder / current sensor check | Critical error |
| Encoder | Measurement | Continous bad measurement | Bad control feedback | High level error | Critical error |
| Encoder | Measurement | Implausibility due to out of range measurement | Bad control feedback | Comparison with mechanical limits | Critical error |
| Current Sensor | Power Supply | Broken / disconnected wire | Torque open loop | Control output and encoder / current sensor check | Critical error |
| Current Sensor | Measurement | Short circuit to VCC/GND | Bad control feedback | Sensor with 0 A offset, GND/VCC detected by Controller | Critical error |

**Table 6.5.** Failure Modes and Effects Analysis

| Item | Category | Failure | Consequences | Detection | Handling |
|---|---|---|---|---|---|
| Current Sensor | Measurement | Continuous bad measurement | Bad control feedback | High-level error | Critical error |
| Torque Sensor | Power Supply | Broken / disconnected wire | Steering wheel torque open loop | Control output and encoder / current / torque sensor check | Critical error |
| Torque Sensor | Measurement | Short circuit to VCC/GND | Bad control feedback | Sensor with 0 A offset, GND/VCC detected by Controller | Critical error |
| Torque Sensor | Measurement | Continuous bad measurement | Bad control feedback | High level error | Critical error |

The vast majority of potential errors identified are non-recoverable since they would be caused by malfunctioning or broken hardware, which would need a system disassembly. Nevertheless, the system could recover from configuration-related errors once they were remedied.

Periodically, concretely each 100 ms, the controller checks and corroborates that there are not any errors, using, as mentioned, the control output generated, the reference and the sensors values. If an error is present, a Safe-State in which the motor supply is disconnected is entered.

### 6.8.2 Program structure and Real-Time analysis

The program structure and real-time capabilities are as important as the controller itself in embedded applications. If the computing unit cannot execute every instruction in its respective time, the control will start to lose performance and even safety could be compromised. Due to the nature of the application, code fragments need to be executed at different time rates in both position and torque control loops. Therefore, a time-interrupt-based program is proposed. The chronological execution of the control loop is now presented:

**Algorithm 1:** Control loop

```
while No errors do
    if Received CAN message then
        Read new CAN messages with reference
    end
    if Position control then
        if t ≥ 1ms then
            Read position sensor
            Compute position control and send command to H-Bridge
        end
        if t ≥ 10ms then
            Send status to higher-level control through CAN
        end
        if t ≥ 100ms then
            Read current and torque sensors and check for errors
        end
    end
    if Current control then
        if t ≥ 1ms then
            Read position, current and torque sensors
            Compute torque control and send command to H-Bridge
            Send status to higher-level control through CAN
        end
        if t ≥ 100ms then
            Check for errors
        end
    end
end
```

where $t$ is asynchronously updated through timed interruptions.

Nevertheless, the control loop, either position or torque, is only a part of the whole program, which is now represented through a State Machine.

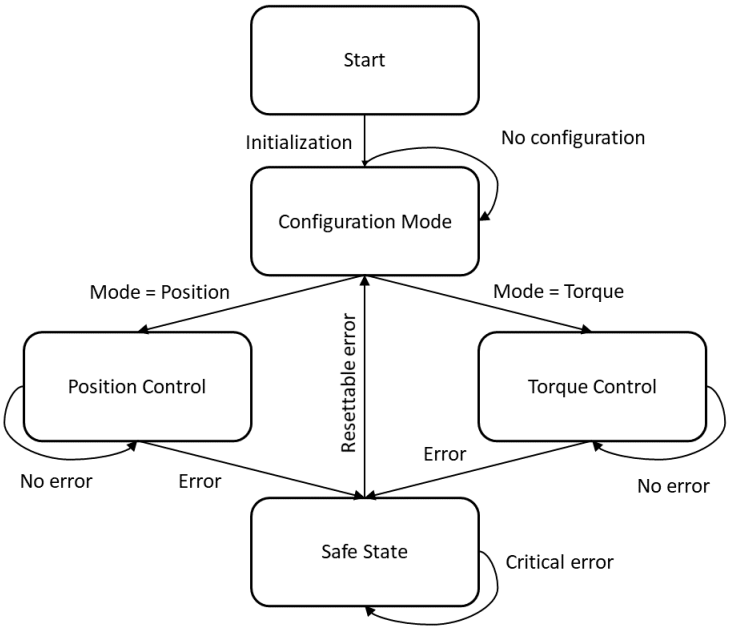


**Figure 6.42.** State Machine

In order to ensure that the MicroAutoBox is capable of executing the control loop within the fixed time periods, a code execution time analysis is made. The methodology used to carry out this test was to measure each of the code fragments' average execution time and analyse the worst-case scenario.

**Table 6.6.** Execution time of code fragments

| **Fragment** | **Average Time ($\mu s$)** |
|---|---|
| CAN reading | 0.128 |
| Current and torque sensors reading | 7.95 |
| Position sensor reading | 3.88 |
| Position control | 1.45 |
| Torque control | 2.2 |
| Send command to H-Bridge | 0.524 |
| Send status to higher-level control | 0.12 |
| Check for errors | 1.88 |

The processor runs at an 900 MHz frequency, which, looking at Table 6.6, is enough to guarantee deadlines. The high-control updates the reference through CAN at a 10 ms rate. This means that only one message would be received within the 1 ms cycle of the control loop in the worst-case scenario. In case the error checking routine is also executed in that cycle, the entire execution time would be the following:

$$t_{position} = 0.000128{+}0.00795 + 0.00388 + 0.00145 + 0.000524 + 0.00012 + 0.00167 = 0.0159\ ms \leq 1\ ms \tag{6.13}$$

$$t_{torque} = 0.000128{+}0.00795 + 0.00388 + 0.00220 + 0.000524 + 0.00012 + 0.00167 = 0.0167\ ms \leq 1\ ms \tag{6.14}$$

Both control loops have a maximum execution time around five times smaller than the deadline, meaning that the system's deadlines are guaranteed.

# 7 Methodology

The following chapter is a breakdown of the tasks carried out during the project and their time allocation.

## 7.1 Task description

The development of this project can be broken down into the following phases or tasks:

1. **Definition of the project requirements:** In this phase, both the objectives and the scope of the project are established, based on the functionalities to be achieved, as well as a first iteration of the time horizon.
    - Human resources: Junior engineer, project manager.
    - Technical resources: PC, Microsoft Office
    - Duration: 1 week
2. **Analysis of the State-of-the-Art:** During this phase, research for similar and related works on the current State-of-the-Art in literature is carried out.
    - Human resources: Junior engineer.
    - Technical resources: PC, Mendeley Reference Manager
    - Duration: 2 weeks
3. **Hardware selection and conditioning:** This stage comprises the selection and purchase of the needed hardware, as well as its conditioning and commissioning.
    - Human resources: Junior engineer.
    - Technical resources: PC, MicroAutoBox II, steering shaft, Kvaser CAN Analyser, dynamometric wrench, wires, protoboard, electronic components.
    - Duration: 2 weeks

4. **Motor modelling:** In this phase, the motor modelling and the acquisition of its mathematical model explained in section 6.5 is carried out.

    - Human resources: Junior engineer.
    - Technical resources: PC, MicroAutoBox II, MATLAB, steering shaft, steering wheel, Kvaser CAN Analyser, wires, protoboard, electronic components.
    - Duration: 2 weeks

5. **Development of position control:** The first iteration of the position control was developed during this stage, including preliminary validation tests with artificial references.

    - Human resources: Junior engineer.
    - Technical resources: PC, MicroAutoBox II, MATLAB, steering shaft, steering wheel, Kvaser CAN Analyser, wires, protoboard, electronic components.
    - Duration: 2 weeks

6. **Development of torque control:** Includes the development and validation of the torque control, as well as the aforementioned hardware problems.

    - Human resources: Junior engineer.
    - Technical resources: PC, MicroAutoBox II, MATLAB, steering shaft, steering wheel, Kvaser CAN Analyser, wires, protoboard, electronic components.
    - Duration: 5 weeks

7. **FMEA analysis:** Comprises the elaboration of the Failure Mode and Effects Analysis.
    - Human resources: Junior engineer.
    - Technical resources: PC, Microsoft Office.
    - Duration: 1 week
8. **Validation tests with Dynacar:** This phase refers to the more realistic tests carried out using the in-house Dynacar Simulator.
    - Human resources: Junior engineer.
    - Technical resources: PC, MicroAutoBox II, MATLAB, Dynacar, steering shaft, steering wheel, Kvaser CAN Analyser, wires, protoboard, electronic components.
    - Duration: 2 weeks
9. **FMEA and Real-Time analysis:** During this stage, the FMEA considerations are implemented and the Real-Time analysis is carried out.
    - Human resources: Junior engineer.
    - Technical resources: PC, MicroAutoBox II, MATLAB, Kvaser CAN analyser.
    - Duration: 4 weeks
10. **Documentation writing:** This phase runs parallel to the aforementioned phases and covers almost the entire duration of the project. Each of the developments carried out in the previously mentioned phases is documented in this phase.
    - Human resources: Junior engineer.
    - Technical resources: PC, Mendeley Reference Manager, LATEX editor.
    - Duration: 17 weeks

## 7.2 Gantt chart

The Gantt chart associated with the project phases mentioned above is now presented:

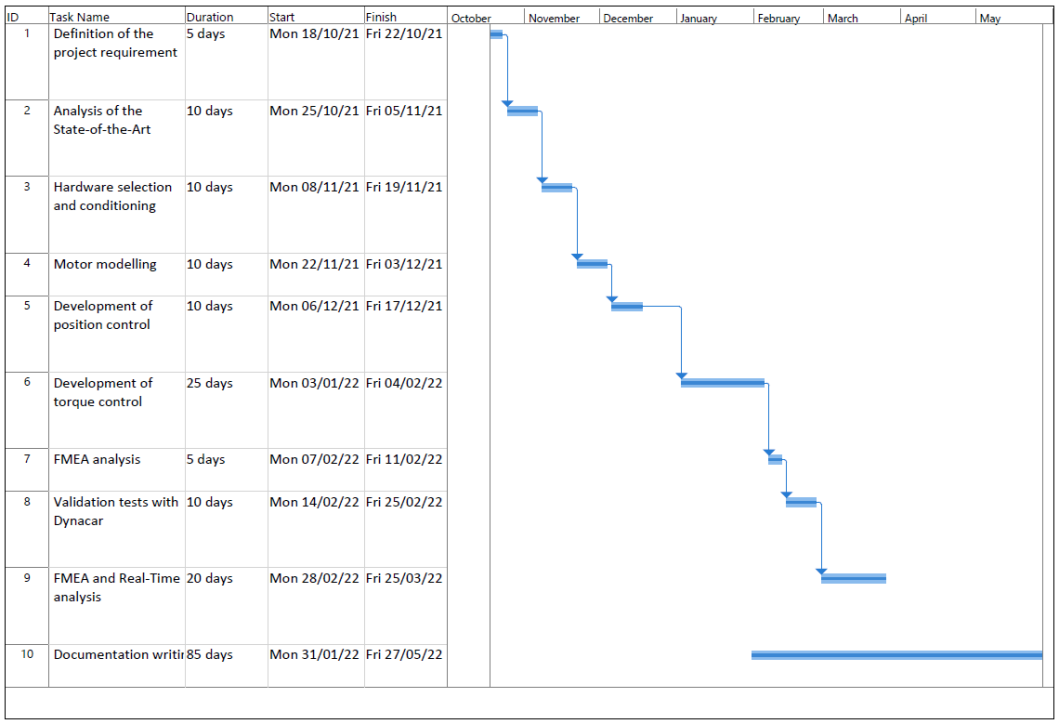

| ID | Task Name | Duration | Start | Finish |
|---|---|---|---|---|
| 1 | Definition of the project requirement | 5 days | Mon 18/10/21 | Fri 22/10/21 |
| 2 | Analysis of the State-of-the-Art | 10 days | Mon 25/10/21 | Fri 05/11/21 |
| 3 | Hardware selection and conditioning | 10 days | Mon 08/11/21 | Fri 19/11/21 |
| 4 | Motor modelling | 10 days | Mon 22/11/21 | Fri 03/12/21 |
| 5 | Development of position control | 10 days | Mon 06/12/21 | Fri 17/12/21 |
| 6 | Development of torque control | 25 days | Mon 03/01/22 | Fri 04/02/22 |
| 7 | FMEA analysis | 5 days | Mon 07/02/22 | Fri 11/02/22 |
| 8 | Validation tests with Dynacar | 10 days | Mon 14/02/22 | Fri 25/02/22 |
| 9 | FMEA and Real-Time analysis | 20 days | Mon 28/02/22 | Fri 25/03/22 |
| 10 | Documentation writi | 85 days | Mon 31/01/22 | Fri 27/05/22 |



**Figure 7.1.** Gantt chart

# 8 Economic aspects

This section breaks down the costs associated with carrying out the Master Thesis. To do this, a breakdown is made into three items: internal hours, amortisations and expenses. A summary is also included with the sum of the three items and the total cost.

**Internal hours:** For the calculation of the cost associated with the number of hours, the working hours associated with a junior engineer are taken into account, as well as those dedicated by the project manager. As mentioned in the previous section, the project lasted 30 weeks, with 5 days worked per week and a daily dedication of 4 hours, which means a total of 600 hours for the junior engineer. The hours of the project manager total 50 in total.

Table 8.1. Economical Aspects: Internal Hours

| Concept | Hours | Cost per hour €/h | Total Cost (€) |
|---|---|---|---|
| Junior Engineer | 600 | 30 | 18 000 |
| Project Manager | 50 | 70 | 3 500 |
| **Total** | | | **21 500** |

**Amortisations:** In addition, it is necessary to include the item corresponding to the amortisations of the resources used during the realisation of the project.

Table 8.2. Economical Aspects: Amortisations

| Concept | Investment (€) | Service life (months) | Use in project (months) | Total Cost (€) |
|---|---|---|---|---|
| PC | 800 | 60 | 8 | 106.67 |
| Microsoft 365 | 126 | 12 | 8 | 84 |
| Power supply | 80 | 72 | 8 | 8.88 |
| MATLAB | 800 | 12 | 8 | 533.33 |
| Altium Designer | 7245 | 12 | 0.5 | 301.88 |
| CAN analyser | 425 | 72 | 8 | 47.22 |
| **Total** | | | | **1 081.98** |

**Expenses:** Next, it is necessary to include the item of expenditure related to the material necessary for the implementation of the project.

Table 8.3. Economical Aspects: Expenses

| Concept | Quantity | Unitary cost €/unit | Total Cost (€) |
|---|---|---|---|
| MicroAutoBox II | 1 | 20000 | 20 000 |
| Sabertooth H-Bridge | 1 | 154 | 154 |
| Cytron H-Bridge | 1 | 55.87 | 55.87 |
| Current Sensor | 1 | 12.72 | 12.72 |
| Steering column | 1 | 70 | 70 |
| Encoder module | 1 | 119 | 119 |
| Steering wheel | 1 | 110 | 110 |
| PCB | 1 | 55.10 | 55.10 |
| Connectors | 1 | 150 | 150 |
| Miscellaneous | 1 | 100 | 100 |
| **Total** | | | **20 826.69** |

**Overall:** Finally, the summary of the total budget is shown, to which is added 5% of the indirect costs of carrying out the project, such as infrastructure or electricity.

Table 8.4. Economical Aspects: Total cost

| Concept | Cost (€) |
|---|---|
| Internal hours | 21 500 |
| Amortisations | 1 081.98 |
| Expenses | 20 826.69 |
| Direct costs | 43 408.67 |
| Indirect costs (5%) | 2 170.43 |
| **Total** | **45 579.1** |

Taking into account both direct costs and indirect costs, the total project budget of the Master Thesis "*Development of an Automated Steering System for Shared Control Applications*" amounts to **45 579.1 €**.

# 9 Conclusions

The course of this TFM has gone through the phases of study, development, and validation of an automated steering system for a Renault Twizy.

In the context of the developments done by the Automated Driving group of Tecnalia Research & Innovation and specifically, one of the future works derived from the PhD Thesis of Dr Mauricio Marcano [47], appropriate steps have been made to enable the implementation and validation of Shared Control algorithms for lateral control of vehicles on real platforms, such as the Renault Twizy. These kinds of light vehicles could serve as a validation platform for non-OEM research institutes for the development of innovative solutions in the field of automated driving, taking advantage of their simplified and accessible design, as well as their reduced cost.

Both low-level position and torque control have been developed starting from an Electronic Power Steering of a commercial Renault Clio. Indeed, this configurable duality facilitates the deployment on the same platform of position-based and torque-based algorithms in a matter of seconds. Thus, it adds flexibility to the vehicle possibilities.

During the modelling stage, it was concluded that even though the efforts to develop a parametric model of the mechanical assembly were unsuccessful, the grey-box model estimated by an optimization process achieved a significantly high correlation. This enabled an analytic design of the controller, as well as a stability study. The comparison between the model and the actual experiments corroborated the quality of the model.

Both position and torque controls are meant to serve as a low-level control for more complex MPC-based algorithms such as the aforementioned shared control or advanced trajectory followers. This implies low sample times, real-time capabilities and high performance following the reference. Nevertheless, in the specific case of torque control, human comfort when handling the steering wheel must also be considered, which leads to the need to find a middle ground.

Finally, validation tests were done using adjustable clamps to simulate different friction levels and, ultimately, a vehicle dynamics simulator that provided more realistic control references.

In the context of the relationship with the Master's syllabus, concepts related to the control branch have been mainly worked out, including automatic control, digital control, modelling and simulation, among others.

To extend the content of this Master Thesis, two future works are proposed. The automated steering system has been validated in HiL simulations but is yet to be assembled and tested on the vehicle. With a high probability, this will lead to the need to adjust both controllers. The other future work proposed corresponds to the substitution of the MicroAutoBox by a smaller commercial automotive ECU, which could elevate the reliability and robustness of the system.

# Bibliography


[1]World Health Organization. *Global status report on road safety*. World Health Organization, 2018 (cit. on p. 17).

[2]Kiichi Yamada, Yumie Minakami, and Keisuke Suzuki. „Analytical Study of Human Errors causing Traffic Accidents from the view point of Consciousness Transition“. In: *IFAC Proceedings Volumes* 41.2 (2008). 17th IFAC World Congress, pp. 8526–8531 (cit. on p. 17).

[3]European Commission. *The European Green Deal*. 2019 (cit. on p. 17).

[4]Panayotis Christidis and J. Nicolás Ibañez. *Measuring road congestion*. European Commission - Institute for Prospective Technological Studies, 2012 (cit. on p. 17).

[5]Francisco Núñez, Elías Albornoz, Javier León, and Antonio Zumelzu. „Socially sustainable mobility: Strategic analysis to identify accessibility barriers“. In: *Sustainable Cities and Society* 76 (2022), p. 103420 (cit. on p. 17).

[6]APUR. *Impacts and potential benefits of autonomous vehicles: From an international context to Grand Paris*. Atelier Parisien d'Urbanisme, 2018 (cit. on p. 18).

[7]Miranda A. Schreurs and Sibyl D. Steuwer. „Autonomous Driving - Political, Legal, Social, and Sustainability Dimensions“. In: *Autonomes Fahren: Technische, rechtliche und gesellschaftliche Aspekte*. Ed. by Markus Maurer, J. Christian Gerdes, Barbara Lenz, and Hermann Winner. Berlin, Heidelberg: Springer Berlin Heidelberg, 2015, pp. 151–173 (cit. on p. 18).

[8]Klaus Bengler, Klaus Dietmayer, Berthold Farber, et al. „Three decades of driver assistance systems: Review and future perspectives“. In: *IEEE Intelligent Transportation Systems Magazine* 6 (4 Dec. 2014), pp. 6–22 (cit. on pp. 18–20).

[9]Bern Grush. „Automated vehicles - virtue or vice?“ In: 2016 (cit. on p. 18).

[10]SAE INTERNATIONAL. *Taxonomy and Definitions for Terms Related to Driving Automation Systems for On-Road Motor Vehicles*. 2014 (cit. on p. 18).

[11]SAE INTERNATIONAL. *Taxonomy and Definitions for Terms Related to Driving Automation Systems for On-Road Motor Vehicles*. 2021 (cit. on pp. 18, 19, 24).

[12]Dominique Gruyer, Valentin Magnier, Karima Hamdi, et al. „Perception, information processing and modeling: Critical stages for autonomous driving applications“. In: *Annual Reviews in Control* 44 (2017), pp. 323–341 (cit. on p. 19).

[13]Matteo Rizzi, Anders Kullgren, and Claes Tingvall. „Injury crash reduction of low-speed Autonomous Emergency Braking (AEB) on passenger cars“. In: *Proc. of IRCOBI Conference on Biomechanics of Impacts*. 2014, pp. 14–73 (cit. on p. 19).

[14]Anton van Zanten and Friedrich Kost. „Bremsenbasierte assistenzfunktionen“. In: *Handbuch Fahrerassistenzsysteme*. Springer, 2009, pp. 356–394 (cit. on p. 19).

[15]Masami Aga and Akio Okada. „Analysis of vehicle stability control (VSC)'s effectiveness from accident data“. In: *Proceedings: International Technical Conference on the Enhanced Safety of Vehicles*. Vol. 2003. National Highway Traffic Safety Administration. 2003, 7–p (cit. on p. 20).

[16]*REGULATION (EU) 2019/2144 OF THE EUROPEAN PARLIAMENT AND OF THE COUNCIL of 27 November 2019* (cit. on p. 20).

[17]E.D. Dickmanns, B. Mysliwetz, and T. Christians. „An integrated spatio-temporal approach to automatic visual guidance of autonomous vehicles“. In: *IEEE Transactions on Systems, Man, and Cybernetics* 20.6 (1990), pp. 1273–1284 (cit. on p. 21).

[18]J. Hellaker. „PROMETHEUS - Strategy“. In: *Vehicle Electronics in the 90's: Proceedings of the International Congress on Transportation Electronics*. 1990, pp. 195–199 (cit. on p. 21).

[19]Keshav Bimbraw. „Autonomous cars: Past, present and future a review of the developments in the last century, the present scenario and the expected future of autonomous vehicle technology“. In: *2015 12th International Conference on Informatics in Control, Automation and Robotics (ICINCO)*. Vol. 01. 2015, pp. 191–198 (cit. on p. 21).

[20]D. Pomerleau and T. Jochem. „Rapidly adapting machine vision for automated vehicle steering“. In: *IEEE Expert* 11.2 (1996), pp. 19–27 (cit. on p. 21).

[21]Enrique Martí, Miguel Ángel De Miguel, Fernando García, and Joshué Pérez. „A Review of Sensor Technologies for Perception in Automated Driving“. In: *IEEE Intelligent Transportation Systems Magazine* 11 (4 Dec. 2019), pp. 94–108 (cit. on p. 21).

[22]Sebastian Thrun, Mike Montemerlo, Hendrik Dahlkamp, et al. „Stanley: The robot that won the DARPA Grand Challenge“. In: *Journal of Field Robotics* 23 (9 Sept. 2006), pp. 661–692 (cit. on p. 21).

[23]Julius Ziegler, Philipp Bender, Markus Schreiber, et al. „Making Bertha Drive—An Autonomous Journey on a Historic Route“. In: *IEEE Intelligent Transportation Systems Magazine* 6.2 (2014), pp. 8–20 (cit. on p. 21).

[24]Joseph Funke, Paul Theodosis, Rami Hindiyeh, et al. „Up to the limits: Autonomous Audi TTS“. In: *2012 IEEE Intelligent Vehicles Symposium*. IEEE. 2012, pp. 541–547 (cit. on p. 22).

[25]Tushar Goel, Jonathan Y Goh, and J Christian Gerdes. „Opening new dimensions: Vehicle motion planning and control using brakes while drifting“. In: *2020 IEEE Intelligent Vehicles Symposium (IV)*. IEEE. 2020, pp. 560–565 (cit. on p. 22).

[26]Sirish Srinivasan, Sebastian Nicolas Giles, and Alexander Liniger. „A holistic motion planning and control solution to challenge a professional racecar driver“. In: *IEEE Robotics and Automation Letters* 6.4 (2021), pp. 7854–7860 (cit. on p. 22).

[27]Alexander Wischnewski, Maximilian Geisslinger, Johannes Betz, et al. „Indy Autonomous Challenge-Autonomous Race Cars at the Handling Limits“. In: *12th International Munich Chassis Symposium 2021*. Springer. 2022, pp. 163–182 (cit. on p. 22).

[28]Stephen Ridella. *ODI RESUME MANUFACTURER & PRODUCT INFORMATION FAILURE REPORT SUMMARY*. National Highway Traffic Safety Administration (NHTSA), 2016 (cit. on p. 22).

[29]Andrew J. Hawkins. *Google's 'worst' self-driving accident was still a human's fault*. 2016. URL: https://www.theverge.com/2016/9/26/13062214/google-self-driving-car-crash-accident-fault (visited on June 8, 2022) (cit. on p. 22).

[30]Peter Moertl. „Human-Systems Integration for Driving Automation Systems: Holistic Approach for Driver Role Integration and Automation Allocation for European Mobility Needs". In: *HCI in Mobility, Transport, and Automotive Systems. Automated Driving and In-Vehicle Experience Design*. Ed. by Heidi Krömker. Cham: Springer International Publishing, 2020, pp. 78–88 (cit. on pp. 24, 25).

[31]HADRIAN. *HADRIAN Project website*. 2019. URL: https://hadrianproject.eu/ (visited on June 1, 2022) (cit. on pp. 24, 25).

[32]M. Kyriakidis, J. C. F. de Winter, N. Stanton, et al. „A human factors perspective on automated driving". In: *Theoretical Issues in Ergonomics Science* 20.3 (2019), pp. 223–249. eprint: https://doi.org/10.1080/1463922X.2017.1293187 (cit. on p. 24).

[33]Jork Stapel, Freddy Antony Mullakkal-Babu, and Riender Happee. „Automated driving reduces perceived workload, but monitoring causes higher cognitive load than manual driving". In: *Transportation Research Part F: Traffic Psychology and Behaviour* 60 (2019), pp. 590–605 (cit. on p. 24).

[34]William Payre, Julien Cestac, and Patricia Delhomme. „Fully automated driving: Impact of trust and practice on manual control recovery". In: *Human factors* 58.2 (2016), pp. 229–241 (cit. on p. 24).

[35]Neville A Stanton. „Thematic issue: driving automation and autonomy". In: *Theoretical Issues in Ergonomics Science* 20.3 (2019), pp. 215–222 (cit. on p. 24).

[36]Daniel Damböck and Klaus Bengler. „Übernahmezeiten beim hochautomatisierten Fahren". In: *5. Tagung Fahrerassistenz*. 2012 (cit. on p. 24).

[37]Paolo Pretto, Norah Joana Neuhuber, and Peter Moertl. „Fluid interface concept for automated driving". English. In: *HCI in Mobility, Transport, and Automotive Systems. Automated Driving and In-Vehicle Experience Design - 2nd International Conference, MobiTAS 2020, Held as Part of the 22nd HCI International Conference, HCII 2020, Proceedings*. Ed. by Heidi Krömker. Lecture Notes in Computer Science. HCI International 2020 : 22nd International Conference on Human-Computer Interaction ; Conference date: 19-07-2020 Through 24-07-2020. 2020, pp. 114–130 (cit. on pp. 25, 26).

[38]Alexander G. Mirnig, Mauricio Marcano, Sandra Trösterer, et al. „Workshop on Exploring Interfaces for Enhanced Automation Assistance for Improving Manual Driving Abilities". In: *13th International Conference on Automotive User Interfaces and Interactive Vehicular Applications*. AutomotiveUI '21 Adjunct. Leeds, United Kingdom: Association for Computing Machinery, 2021, 178–181 (cit. on p. 25).

[39]Myriam Vaca-Recalde, Pedro López-Garíca, Javier Echanobe, and Joshué Pérez. „Eyes Detector Approach for Driving Monitoring System for Occluded Faces without using Facial Landmarks". In: *2021 IEEE 17th International Conference on Intelligent Computer Communication and Processing (ICCP)*. 2021, pp. 117–122 (cit. on p. 26).

[40] Myriam E. Vaca-Recalde, Joshué Pérez, and Javier Echanobe. „Driver Monitoring System Based on CNN Models: An Approach for Attention Level Detection“. In: vol. 12490 LNCS. Springer Science and Business Media Deutschland GmbH, 2020, pp. 575–583 (cit. on p. 26).

[41] Marios Sekadakis, Christos Katrakazas, Erika Santuccio, Peter Mörtl, and George Yannis. „Key Performance Indicators for safe fluid interactions within automated vehicles“. In: *10 International Congress of Transportation Research (ICTR)*. 2021 (cit. on p. 26).

[42] Harsh Sanghavi, Myounghoon Jeon, Chihab Nadri, et al. „Multimodal Takeover Request Displays for Semi-automated Vehicles: Focused on Spatiality and Lead Time“. In: vol. 12791 LNCS. Springer Science and Business Media Deutschland GmbH, 2021, pp. 315–334 (cit. on p. 26).

[43] Peter Moertl, Elisabeth Shi, Nikolai Ebinger, et al. *Toward Integrated Automation Status and Alerting Dis-play Management Systems for Vehicles*. 2021 (cit. on p. 26).

[44] Myriam E. Vaca-Recalde, Mauricio Marcano, Joseba Sarabia, et al. „A Fluid-HMI Approach for Haptic Steering Shared Control for the HADRIAN Project“. In: vol. 12212 LNCS. Springer, 2020, pp. 417–428 (cit. on p. 26).

[45] Mauricio Marcano, Sergio Diaz, Myriam Vaca, Joshué Pérez, and Eloy Irigoyen. „Shared Control Framework and Application for European Research Projects“. In: vol. 1268 AISC. Springer Science and Business Media Deutschland GmbH, 2021, pp. 657–666 (cit. on p. 26).

[46] Joseba Sarabia, Mauricio Marcano, Joshué Pérez Rastelli, Sergio Díaz Briceño, and Asier Zubizarreta. *Estudio preliminar de los métodos de evaluación del control compartido*. Aug. 2021 (cit. on p. 26).

[47] Mauricio A Marcano Sandoval. „Shared Control Strategies for Automated Vehicles“. University of the Basque Country, 2022 (cit. on pp. 26, 29, 35–38, 43, 93).

[48] Steffen Jochum, Lotte Saupp, Jan Bavendiek, Christopher Brockmeier, and Lutz Eckstein. „Investigating Kinematic Parameters of a Turning Seat as a Haptic and Kinesthetic HMI to Support the Take-Over Request in Automated Driving“. In: *International Conference on Applied Human Factors and Ergonomics*. Springer. 2021, pp. 301–307 (cit. on p. 26).

[49] Joseba Sarabia, José A. Matute-Peaspan, and Asier Zubizarreta. „Caracterización de los sistemas de actuación para vehículos altamente automatizados“. In: Universidade da Coruna, Aug. 2019, pp. 596–603 (cit. on p. 26).

[50] David González, Joshué Pérez, Vicente Milanés, and Fawzi Nashashibi. „A Review of Motion Planning Techniques for Automated Vehicles“. In: *IEEE Transactions on Intelligent Transportation Systems* 17 (4 Apr. 2016), pp. 1135–1145 (cit. on pp. 28, 29, 43).

[51] Ray Lattarulo, Daniel Heß, and Joshue Pérez. *A Linear Model Predictive Planning Approach for Overtaking Manoeuvres Under Possible Collision Circumstances; A Linear Model Predictive Planning Approach for Overtaking Manoeuvres Under Possible Collision Circumstances*. 2018 (cit. on p. 28).

[52] Ray Alejandro Lattarulo Arias. „Validation Of Trajectory Planning Strategies For Automated Driving Under Cooperative, Urban, And Interurban Scenarios“. University of the Basque Country, 2019 (cit. on p. 28).

[53] Jose Angel Matute Peaspan. „Design and validation of decision and control systems in Automated Driving“. University of the Basque Country, 2021 (cit. on p. 29).

[54]Ray Lattarulo, Joshué Pérez, and Martin Dendaluce. „A complete framework for developing and testing automated driving controllers“. In: *IFAC-PapersOnLine* 50.1 (2017), pp. 258–263 (cit. on p. 29).

[55]Ray Lattarulo, Carlos Hidalgo, Asier Arizala, and Joshue Perez. „AUDRIC2: A Modular and Highly Interconnected Automated Driving Framework Focus on Decision Making and Vehicle Control“. In: *2021 IEEE International Intelligent Transportation Systems Conference (ITSC)*. 2021, pp. 763–769 (cit. on pp. 29, 43, 78).

[56]F. Flemisch, D. A. Abbink, M. Itoh, M. P. Pacaux-Lemoine, and G. Weßel. „Joining the blunt and the pointy end of the spear: towards a common framework of joint action, human–machine cooperation, cooperative guidance and control, shared, traded and supervisory control“. In: *Cognition, Technology and Work* 21 (4 Nov. 2019), pp. 555–568 (cit. on p. 35).

[57]Canjun Yang, Yuanchao Zhu, and Yanhu Chen. „A Review of Human–Machine Cooperation in the Robotics Domain“. In: *IEEE Transactions on Human-Machine Systems* (2021) (cit. on p. 35).

[58]David A. Abbink, Tom Carlson, Mark Mulder, et al. „A topology of shared control systems-finding common ground in diversity“. In: *IEEE Transactions on Human-Machine Systems* 48 (5 Oct. 2018), pp. 509–525 (cit. on pp. 35, 36).

[59]Joost De Winter, Sebastiaan Petermeijer, and David Abbink. *Shared control versus traded control in driving: A debate around automation pitfalls*. 2022 (cit. on pp. 35, 36).

[60]Mustafa Suphi Erden and Bobby Marić. „Assisting manual welding with robot“. In: *Robotics and Computer-Integrated Manufacturing* 27.4 (2011), pp. 818–828 (cit. on p. 35).

[61]David A. Abbink, Mark Mulder, and Erwin R. Boer. „Haptic shared control: Smoothly shifting control authority?“ In: *Cognition, Technology and Work* 14 (1 Mar. 2012), pp. 19–28 (cit. on p. 36).

[62]Joost CF De Winter, Riender Happee, Marieke H Martens, and Neville A Stanton. „Effects of adaptive cruise control and highly automated driving on workload and situation awareness: A review of the empirical evidence“. In: *Transportation research part F: traffic psychology and behaviour* 27 (2014), pp. 196–217 (cit. on p. 36).

[63]Mauricio Marcano, Sergio Díaz, Joshue Perez, and Eloy Irigoyen. „A Review of Shared Control for Automated Vehicles: Theory and Applications“. In: *IEEE Transactions on Human-Machine Systems* 50 (6 Dec. 2020), pp. 475–491 (cit. on pp. 36–38).

[64]Frank O Flemisch, Catherine A Adams, Sheila R Conway, et al. *The H-Metaphor as a guideline for vehicle automation and interaction*. Tech. rep. 2003 (cit. on p. 36).

[65]Mark Mulder, Max Mulder, MM van Paassen, et al. „Car-following support with haptic gas pedal feedback“. In: *Proceedings of IFAC Symposium on Analysis, Design, and Evaluation of Human-Machine Systems*. 2004 (cit. on p. 37).

[66]Ziya Ercan, Ashwin Carvalho, H Eric Tseng, Metin Gökaşan, and Francesco Borrelli. „A predictive control framework for torque-based steering assistance to improve safety in highway driving“. In: *Vehicle system dynamics* 56.5 (2018), pp. 810–831 (cit. on p. 37).

[67] Xuewu Ji, Kaiming Yang, Xiaoxiang Na, Chen Lv, and Yahui Liu. „Shared Steering Torque Control for Lane Change Assistance: A Stochastic Game-Theoretic Approach“. In: *IEEE Transactions on Industrial Electronics* 66 (4 Apr. 2019), pp. 3093–3105 (cit. on pp. 37, 39).

[68] Mauricio Marcano, Fabio Tango, Joseba Sarabia, et al. „From the concept of being “the boss” to the idea of being “a team”: The adaptive co-pilot as the enabler for a new cooperative framework“. In: *Applied Sciences (Switzerland)* 11 (15 Aug. 2021) (cit. on p. 37).

[69] Philippe Morignot, Joshué Pérez Rastelli, and Fawzi Nashashibi. „Arbitration for balancing control between the driver and ADAS systems in an automated vehicle: Survey and approach“. In: *2014 IEEE Intelligent Vehicles Symposium Proceedings*. IEEE. 2014, pp. 575–580 (cit. on p. 38).

[70] Christian Löper, Johann Kelsch, and Frank Ole Flemisch. „Kooperative, manöverbasierte Automation und Arbitrierung als Bausteine für hochautomatisiertes Fahren“. In: (2008) (cit. on p. 38).

[71] Sterling J Anderson, James M Walker, and Karl Iagnemma. „Experimental performance analysis of a homotopy-based shared autonomy framework“. In: *IEEE Transactions on Human-Machine Systems* 44.2 (2014), pp. 190–199 (cit. on p. 38).

[72] Jun Liu, Hong Chen, Hongyan Guo, Linhuan Song, and Yunfeng Hu. „Moving horizon shared steering strategy for intelligent vehicle based on potential-hazard analysis“. In: *IET Intelligent Transport Systems* 13.3 (2019), pp. 541–550 (cit. on p. 38).

[73] Mauricio Marcano, Sergio Díaz, Jose A Matute, Eloy Irigoyen, and Joshué Pérez. *A cascade steering shared controller with dual-level dynamic authority*. 2020 (cit. on p. 38).

[74] Avinash Balachandran, Matthew Brown, Stephen M. Erlien, and J. Christian Gerdes. „Predictive haptic feedback for obstacle avoidance based on model predictive control“. In: *IEEE Transactions on Automation Science and Engineering* 13 (1 Jan. 2016), pp. 26–31 (cit. on p. 38).

[75] Nicoleta Minoiu Enache, Saïd Mammar, Mariana Netto, and Benoit Lusetti. „Driver steering assistance for lane-departure avoidance based on hybrid automata and composite Lyapunov function“. In: *IEEE Transactions on Intelligent Transportation Systems* 11 (1 Mar. 2010), pp. 28–39 (cit. on p. 38).

[76] Franck Mars, Mathieu Deroo, and Jean Michel Hoc. „Analysis of human-machine cooperation when driving with different degrees of haptic shared control“. In: *IEEE Transactions on Haptics* 7 (3 July 2014), pp. 324–333 (cit. on p. 38).

[77] Amir Benloucif, Anh Tu Nguyen, Chouki Sentouh, and Jean Christophe Popieul. „Cooperative trajectory planning for haptic shared control between driver and automation in highway driving“. In: *IEEE Transactions on Industrial Electronics* 66 (12 Dec. 2019), pp. 9846–9857 (cit. on p. 38).

[78] Panithi Phetnok, Aphilak Lonklang, and Suradet Tantrairatn. „Implementation of Steering-by-Wire Control System for Electric Golf Cart“. In: 2019 (cit. on p. 40).

[79] Arvind Goyal and Ayushi Thakur. „An Overview of Drive by Wire Technology for Automobiles“. In: 2019 (cit. on pp. 40, 41).

[80]Vicente Milanés, Joshué Pérez, Enrique Onieva, Carlos González, and Teresa De Pedro. „Electric power controller for steering wheel management in electric cars“. In: 2009, pp. 444–449 (cit. on p. 40).

[81]Elizabeth A Bretz. „By-wire cars turn the corner“. In: *IEEE Spectrum* 38.4 (2001), pp. 68–73 (cit. on p. 40).

[82]Seyed Abolfazl Mortazavizadeh, Ahmad Ghaderi, Mohammad Ebrahimi, and Masood Hajian. „Recent developments in the vehicle steer-by-wire system“. In: *IEEE Transactions on Transportation Electrification* 6.3 (2020), pp. 1226–1235 (cit. on p. 41).

[83]Tomas Pawlenka and Jaromir Skuta. „Electronic steering with force feedback“. In: Institute of Electrical and Electronics Engineers Inc., May 2019 (cit. on p. 41).

[84]Paul Yih and J Christian Gerdes. „Modification of vehicle handling characteristics via steer-by-wire“. In: *IEEE transactions on control systems technology* 13.6 (2005), pp. 965–976 (cit. on p. 41).

[85]Chao Huang, Fazel Naghdy, and Haiping Du. „Fault tolerant sliding mode predictive control for uncertain steer-by-wire system“. In: *IEEE Transactions on Cybernetics* 49 (1 Jan. 2019), pp. 261–272 (cit. on p. 41).

[86]Miguel Angel Sotelo. „Lateral control strategy for autonomous steering of Ackerman-like vehicles“. In: *Robotics and Autonomous Systems* 45 (3-4 Dec. 2003), pp. 223–233 (cit. on p. 41).

[87]Joshué Pérez, Vicente Milanés, and Enrique Onieva. „Cascade architecture for lateral control in autonomous vehicles“. In: *IEEE Transactions on Intelligent Transportation Systems* 12.1 (2011), pp. 73–82 (cit. on p. 41).

[88]Myung-Wook Park, Sang-Woo Lee, and Woo-Yong Han. „Development of lateral control system for autonomous vehicle based on adaptive pure pursuit algorithm“. In: *2014 14th International Conference on Control, Automation and Systems (ICCAS 2014)*. IEEE. 2014, pp. 1443–1447 (cit. on p. 41).

[89]Pan Zhao, Jiajia Chen, Yan Song, et al. „Design of a control system for an autonomous vehicle based on adaptive-pid“. In: *International Journal of Advanced Robotic Systems* 9.2 (2012), p. 44 (cit. on p. 41).

[90]Xinyu Wang, Mengyin Fu, Hongbin Ma, and Yi Yang. „Lateral control of autonomous vehicles based on fuzzy logic“. In: *Control Engineering Practice* 34 (2015), pp. 1–17 (cit. on p. 41).

[91]AM Harsha S Abeykoon and Hasala R Senevirathne. „Disturbance observer based current controller for a brushed DC motor“. In: *2012 IEEE 6th International Conference on Information and Automation for Sustainability*. IEEE. 2012, pp. 47–52 (cit. on p. 41).

[92]Dounia Saifia, Mohammed Chadli, Hamid Reza Karimi, and Salim Labiod. „Fuzzy control for electric power steering system with assist motor current input constraints“. In: *Journal of the Franklin Institute* 352.2 (2015), pp. 562–576 (cit. on p. 41).

[93]Christopher Dunkel, Toralf Trautmann, and Sven Eckelmann. „Adaption eines Versuchsträgers und Entwicklung von Funktionsprototypen für automatisierte Fahrfunktionen“. Hochschule für Technik und Wirtschaft Dresden, 2017 (cit. on pp. 46, 47).

[94]LEM Components. *Isolated current and voltage transducers. Characteristics - Applications - Calculations* (cit. on p. 48).

[95]Mathworks. *DC Servo Motor Parameter Estimation*. 2017. URL: https://uk.mathworks.com/help/sldo/ug/dc-servo-motor-parameter-estimation.html (visited on May 7, 2022) (cit. on pp. 57, 58).

[96]Alberto Peña, Iñaki Iglesias, Juan Valera, and A Martin. „Development and validation of Dynacar RT software, a new integrated solution for design of electric and hybrid vehicles“. In: vol. 3. May 2012 (cit. on p. 78).